

Continuity of the path delay operator for dynamic network loading with spillback

Ke Han^{a,*}, Benedetto Piccoli^b, Terry L. Friesz^c^a*Department of Civil and Environmental Engineering, Imperial College London, United Kingdom.*^b*Department of Mathematical Sciences and CCIB, Rutgers University - Camden, USA*^c*Department of Industrial and Manufacturing Engineering, Pennsylvania State University, USA.*

Abstract

This paper establishes the continuity of the path delay operators for *dynamic network loading* (DNL) problems based on the Lighthill-Whitham-Richards model, which explicitly capture vehicle spillback. The DNL describes and predicts the spatial-temporal evolution of traffic flow and congestion on a network that is consistent with established route and departure time choices of travelers. The LWR-based DNL model is first formulated as a system of *partial differential algebraic equations* (PDAEs). We then investigate the continuous dependence of merge and diverge junction models with respect to their initial/boundary conditions, which leads to the continuity of the path delay operator through the *wave-front tracking* methodology and the *generalized tangent vector* technique. As part of our analysis leading up to the main continuity result, we also provide an estimation of the minimum network supply without resort to any numerical computation. In particular, it is shown that gridlock can never occur in a finite time horizon in the DNL model.

Keywords: path delay operator, continuity, dynamic network loading, LWR model, spillback, gridlock

1. Introduction

Dynamic traffic assignment (DTA) is the descriptive modeling of time-varying flows on traffic networks consistent with traffic flow theory and travel choice principles. DTA models describe and predict departure rates, departure times and route choices of travelers over a given time horizon. It seeks to describe the dynamic evolution of traffic in networks in a fashion consistent with the fundamental notions of traffic flow and travel demand; see Peeta and Ziliaskopoulos (2001) for some review on DTA models and recent developments. *Dynamic user equilibrium* (DUE) of the open-loop type, which is one type of DTA, remains a major modern perspective on traffic modeling that enjoys wide scholarly support. It captures two aspects of driving behavior quite well: departure time choice and route choice (Friesz et al., 1993). Within the DUE model, travel cost for the same trip purpose is identical for all utilized route-and-departure-time choices. The relevant notion of travel cost is *effective travel delay*, which is a weighted sum of actual travel time and arrival penalties.

In the last two decades there have been many efforts to develop a theoretically sound formulation of dynamic network user equilibrium that is also a canonical form acceptable to scholars and practitioners alike. There are two essential components within the DUE models: (1) the mathematical expression of Nash-like equilibrium conditions;

*Corresponding author

Email addresses: k.han@imperial.ac.uk (Ke Han), piccoli@camden.rutgers.edu (Benedetto Piccoli), tfriesz@psu.edu (Terry L. Friesz)

and (2) a network performance model, which is, in effect, an embedded *dynamic network loading* (DNL) problem. The DNL model captures the relationships among link entry flow, link exit flow, link delay and path delay for any given set of path departure rates. The DNL gives rise to the notion of *path delay operator*, which is viewed as a mapping from the set of feasible path departure rates to the set of path travel times or, more generally, path travel costs.

Properties of the path delay operator are of fundamental importance to DUE models. In particular, continuity of the delay operators plays a key role in the existence and computation of DUE models. The existence of DUEs is typically established by converting the problem to an equivalent mathematical form and applying some version of Brouwer's fixed-point existence theorem; examples include Han et al. (2013c); Smith and Wisten (1995); Wie et al. (2002) and Zhu and Marcotte (2000). All of these existence theories rely on the continuity of the path delay operator. On the computational side of analytical DUE models, every established algorithm requires the continuity of the delay operator to ensure convergence; an incomplete list of such algorithms include the fixed-point algorithm (Friesz et al., 2013), the route-swapping algorithm (Huang and Lam, 2002), the descent method (Han and Lo, 2003), the projection method (Han and Lo, 2002; Ukkusuri et al., 2012), and the proximal point method (Han et al., 2015a)

It has been difficult historically to show continuity of the delay operator for general network topologies and traffic flow models. Over the past decade, only a few continuity results were established for some specific traffic flow models. Zhu and Marcotte (2000) use the link delay model (Friesz et al., 1993) to show the continuity of the path delay operator. Their result relies on the *a priori* boundedness of the path departure rates, and is later improved by a continuity result that is free of such an assumption (Han et al., 2012). In Bressan and Han (2013), continuity of the delay operator is shown for networks whose dynamics are described by the LWR-Lax model (Bressan and Han, 2011; Friesz et al., 2013), which is a variation of the LWR model that does not capture vehicle spillback. Their result also relies on the *a priori* boundedness of path departure rates. Han et al. (2013c) consider Vickrey's point queue model (Vickrey, 1969) and show the continuity of the corresponding path delay operator for general networks without invoking the boundedness on the path departure rates.

All of these aforementioned results are established for network performance models that do not capture vehicle spillback. To the best of our knowledge, there has not been any rigorous proof of the continuity result for DNL models that allow queue spillback to be explicitly captured. On the contrary, some existing studies even show that the path travel times may depend discontinuously on the path departure rates, when physical queue models are used. For example, Szeto (2003) uses the cell transmission model and signal control to show that the path travel time may depend on the path departure rates in a discontinuous way. Such a finding suggests that the continuity of the delay operator could very well fail when spillback is present. This has been the major hurdle in showing the continuity or identifying relevant conditions under which the continuity is guaranteed. This paper bridges this gap by articulating these conditions and providing accompanying proof of continuity.

This paper presents, for the first time, a rigorous continuity result for the path delay operator based on the LWR network model, which explicitly captures physical queues and vehicle spillback. In showing the desired continuity, we propose a systematic approach for analyzing the well-posedness of two specific junction models¹: a merge and a diverge model, both originally presented by Daganzo (1995). The underpinning analytical framework employs the *wave-front tracking* methodology (Dafermos, 1972; Holden and Risebro, 2002) and the technique of *generalized tangent vectors* (Bressan, 1993; Bressan et al., 2000). A major portion of our proof involves the analysis of the interactions between kinematic waves and the junctions, which is frequently invoked for the study of well-posedness of junction models; see Garavello and Piccoli (2006) for more details. Such analysis is further complicated by the fact that vehicle turning ratios at a diverge junction are determined endogenously by drivers' route choices within the DNL procedure. As a result, special tools are developed in this paper to handle this unique situation.

As we shall later see, a crucial step of the process above is to estimate and bound from below the minimum network supply, which is defined in terms of local vehicle densities in the same way as in Lebacque and Khoshyaran (1999). In fact, if the supply somewhere tends to zero (that is, when traffic approaches the jam density), the well-posedness of the diverge junction may fail, as we demonstrate in Section 4.2.1. This has also been confirmed by the earlier study of Szeto (2003), where a wave of jam density is triggered by a signal red light and causes spillback at the upstream junction, leading to a jump in the path travel times. Remarkably, in this paper we are able to show that (1) if the supply

¹Well-posedness of a model refers to the property that the behavior of the solution hardly changes when there is a slight change in the initial/boundary conditions.

is bounded away from zero (that is, traffic is bounded away from the jam density), then the diverge junction model is well posed; and (2) the desired boundedness of the supply is a natural consequence of the dynamic network loading procedure that involves only the merge and diverge junction models we study here. This is a highly non-trivial result because it not only plays a role in the continuity proof, but also implies that gridlock can never occur in the network loading procedure in any finite time horizon.

The final continuity result is presented in Section 5.4, following a number of preliminary results set out in previous sections. Although our continuity result is established only for networks consisting of simple merge and diverge nodes, it can be extended to networks with more complex topologies using the procedure of decomposing any junction into several simple merge and diverge nodes (Daganzo, 1995). Moreover, the analytical framework employed by this paper can be invoked to treat other and more general junction topologies and/or merging and diverging rules, and the techniques employed to analyze wave interactions will remain valid.

The main contributions made in this paper include:

- formulation of the LWR-based dynamic network loading (DNL) model with spillback as a system of *partial differential algebraic equations* (PDAEs);
- a continuity result for the path delay operator based on the aforementioned DNL model;
- a novel method for estimating the network supply, which shows that gridlock can never occur within a finite time horizon.

The rest of this paper is organized as follows. Section 2 recaps some essential knowledge and notions regarding the LWR network model and the DNL procedure. Section 3 articulates the mathematical contents of the DNL model by formulating it as a PDAE system. Section 4 introduces the merge and diverge models and establishes their well-posedness. Section 5 provides a final proof of continuity and some discussions. Finally, we offer some concluding remarks in Section 6.

2. LWR-based dynamic network loading

2.1. Delay operator and dynamic network loading

Throughout this paper, the time interval of analysis is a single commuting period expressed as $[0, T]$ for some $T > 0$. We let \mathcal{P} be the set of all paths employed by travelers. For each path $p \in \mathcal{P}$ we define the path departure rate which is a function of departure time $t \in [0, T]$:

$$h_p(\cdot) : [0, T] \rightarrow \mathbb{R}_+$$

where \mathbb{R}_+ denotes the set of non-negative real numbers. Each path departure rate $h_p(t)$ is interpreted as a time-varying path flow measured at the entrance of the first arc of the relevant path, and the unit for $h_p(t)$ is *vehicles per unit time*. We next define $h(\cdot) = \{h_p(\cdot) : p \in \mathcal{P}\}$ to be a vector of departure rates. Therefore, $h = h(\cdot)$ can be viewed as a vector-valued function of t , the departure time ².

The single most crucial ingredient is the path delay operator, which maps a given vector of departure rates h to a vector of path travel times. More specifically, we let

$$D_p(t, h) \quad \forall t \in [t_0, t_f], \quad \forall p \in \mathcal{P}$$

be the path travel time of a driver departing at time t and following path p , given the departure rates h associated with all the paths in the network. We then define the path delay operator $D(\cdot)$ by letting $D(h) = \{D_p(\cdot, h) : p \in \mathcal{P}\}$, which is a vector consisting of time-dependent path travel times $D_p(t, h)$.

²For notation convenience and without causing any confusion, we will sometimes use h instead of $h(\cdot)$ to denote path flow vectors.

2.2. The Lighthill-Whitham-Richards model on networks

We recap the network extension of the LWR model (Lighthill and Whitham, 1955; Richards, 1956), which captures the formation, propagation, and dissipation of spatial queues and vehicle spillback. Discussion provided below relies on general assumptions on the fundamental diagram and the junction model, and involves no *ad hoc* treatment of flow propagation, flow conservation, link delay, or other critical model features.

We consider a road link expressed as a spatial interval $[a, b] \subset \mathbb{R}$. The *partial differential equation* (PDE) representation of the LWR model is the following scalar conservation law

$$\partial_t \rho(t, x) + \partial_x f(\rho(t, x)) = 0 \quad (t, x) \in [0, T] \times [a, b] \quad (2.1)$$

with appropriate initial and boundary conditions, which will be discussed in detail later. Here, $\rho(t, x)$ denotes vehicle density at a given point in the space-time domain. The fundamental diagram $f(\cdot) : [0, \rho^{jam}] \rightarrow [0, C]$ expresses vehicle flow at (t, x) as a function of $\rho(t, x)$, where ρ^{jam} denotes the jam density, and C denotes the flow capacity. Throughout this paper, we impose the following mild assumption on $f(\cdot)$:

(F). The fundamental diagram $f(\cdot)$ is continuous, concave and vanishes at $\rho = 0$ and $\rho = \rho^{jam}$.

An essential component of the network extension of the LWR model is the specification of boundary conditions at a road junction. Derivation of the boundary conditions should not only obey physical realism, such as that enforced by entropy conditions (Garavello and Piccoli, 2006; Holden and Risebro, 1995), but also reflect certain behavioral and operational considerations, such as vehicle turning preferences (Daganzo, 1995), driving priorities (Coclite et al., 2005), and signal controls (Han et al., 2014). Articulation of a junction model is facilitated by the notion of *Riemann Problem*, which is an initial value problem at the junction with constant initial condition on each incident link. There exist a number of junction models that yield different solutions of the same Riemann Problem. In one line of research, an entropy condition is defined based on a minimization/maximization problem (Holden and Risebro, 1995). In another line of research, the boundary conditions are defined using link *demand* and *supply* (Lebacque and Khoshyaran, 1999), which represent the link's sending and receiving capacities. Models following this approach include Daganzo (1995); Jin and Zhang (2003) and Jin (2010). The solution of a Riemann Problem is given by the *Riemann Solver* (RS), to be defined below.

2.2.1. The Riemann Solver

We consider a general road junction J with m incoming roads and n outgoing roads, as shown in Figure 1.

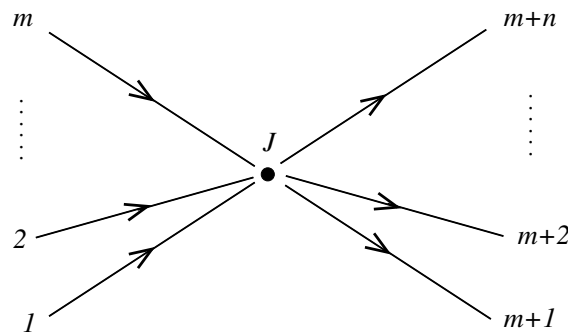


Figure 1: A road junction with m incoming links and n outgoing links.

We denote by I_1, \dots, I_m the incoming links and by I_{m+1}, \dots, I_{m+n} the outgoing links. In addition, for every $i \in \{1, \dots, m+n\}$, the dynamic on I_i is governed by the LWR model

$$\partial_t \rho_i(t, x) + \partial_x f_i(\rho_i(t, x)) = 0 \quad (t, x) \in [0, T] \times [a_i, b_i] \quad (2.2)$$

where link I_i is expressed as the spatial interval $[a_i, b_i]$, and we always use the subscript ' i ' to indicate dependence on the link I_i . The initial condition for this conservation law is

$$\rho_i(0, x) = \hat{\rho}_i(x) \quad x \in [a_i, b_i] \quad (2.3)$$

Notice that the above $(m+n)$ initial value problems are coupled together via the boundary conditions to be specified at the junction. Such a system of coupling equations is commonly analyzed using the Riemann Problem.

Definition 2.1. (Riemann Problem) *The Riemann Problem at the junction J is defined to be an initial value problem on a network consisting of the single junction J with m incoming links and n outgoing links, all extending to infinity, such that the initial densities are constants on each link:*

$$\begin{cases} \rho_i(0, x) \equiv \hat{\rho}_i & x \in (-\infty, b_i], & i \in \{1, \dots, m\} \\ \rho_j(0, x) \equiv \hat{\rho}_j & x \in [a_j, +\infty), & j \in \{m+1, \dots, m+n\} \end{cases}$$

where $\hat{\rho}_k \in [0, \rho_k^{jam}]$ are constants, $k = 1, \dots, m+n$.

A Riemann Solver for the junction J is a mapping that, given any $(m+n)$ -tuple of Riemann initial conditions $(\hat{\rho}_1, \dots, \hat{\rho}_{m+n})$, provides a unique $(m+n)$ -tuple of boundary conditions $(\bar{\rho}_1, \dots, \bar{\rho}_{m+n})$ such that one can solve the initial-boundary value problem for each link, and the resulting solutions constitute a weak entropy solution of the Riemann Problem at the junction³. A precise definition of the Riemann Solver is given as follows.

Definition 2.2. (Riemann Solver) *A Riemann Solver for the junction J with m incoming links and n outgoing links is a mapping*

$$RS : \prod_{k=1}^{m+n} [0, \rho_k^{jam}] \longrightarrow \prod_{k=1}^{m+n} [0, \rho_k^{jam}]$$

$$(\hat{\rho}_1, \dots, \hat{\rho}_{m+n}) \mapsto (\bar{\rho}_1, \dots, \bar{\rho}_{m+n})$$

which relates Riemann initial data $\hat{\rho} = (\hat{\rho}_1, \dots, \hat{\rho}_{m+n})$ to boundary conditions $\bar{\rho} = (\bar{\rho}_1, \dots, \bar{\rho}_{m+n})$, such that the following hold.

- (i) *The solution of the Riemann Problem restricted on each link I_k is given by the solution of the initial-boundary value problem with initial condition $\hat{\rho}_k$ and boundary condition $\bar{\rho}_k$, $k = 1, \dots, m+n$.*
- (ii) *The Rankine-Hugoniot condition (flow conservation) holds:*

$$\sum_{i=1}^m f_i(\bar{\rho}_i) = \sum_{j=m+1}^{m+n} f_j(\bar{\rho}_j) \quad (2.4)$$

- (iii) *The consistency condition holds:*

$$RS[RS[\hat{\rho}]] = RS[\hat{\rho}] \quad (2.5)$$

Three conditions must be satisfied by the Riemann Solver (RS). Item (i) above requires that the boundary condition on each link must be properly given so that the initial value problems not only have well-defined solutions, but these solutions must also be compatible and form a sensible solution at the junction. (2.4) simply stipulates the conservation of flow across the junction. (2.5) is a desirable property and is sometimes referred to as the *invariance property* (Jin, 2010).

Remark 2.3. *For the same Riemann Problem, there exist many Riemann Solvers that satisfy conditions (i)-(iii) above. Despite their varying forms, most existing Riemann Solvers rely on a flow maximization problem at the relevant junction subject to constraints related to turning ratio, right-of-way, or signal controls; see (Coclite et al., 2005; Han et al., 2014; Holden and Risebro, 1995; Jin and Zhang, 2003) and Jin (2010).*

³We refer the reader to Holden and Risebro (1995) for a definition of weak entropy solution at a junction

2.2.2. The link demand and supply

For each link I_i , we let ρ_i^c be the critical density at which the flow is maximized. The demand $D_i(t)$ for incoming links I_i and the supply $S_j(t)$ for outgoing links I_j are defined in terms of the density near the exit and entrance of the link, respectively (Lebacque and Khoshyaran, 1999):

$$D_i(t) = D_i(\rho_i(t, b_i-)) = \begin{cases} C_i & \text{if } \rho_i(t, b_i-) \geq \rho_i^c \\ f_i(\rho_i(t, b_i-)) & \text{if } \rho_i(t, b_i-) < \rho_i^c \end{cases} \quad (2.6)$$

$$S_j(t) = S_j(\rho_j(t, a_j+)) = \begin{cases} C_j & \text{if } \rho_j(t, a_j+) \leq \rho_j^c \\ f_j(\rho_j(t, a_j+)) & \text{if } \rho_j(t, a_j+) > \rho_j^c \end{cases} \quad (2.7)$$

In prose, the demand represents the maximum flow at which cars can be discharged from the incoming link; and the supply represents the maximum flow at which cars can enter the outgoing link. Notice that the demand and supply are both expressed as functions of density, and they are always greater than or equal to the fundamental diagram $f_i(\cdot)$ or $f_j(\cdot)$; see Figure 2 for an illustration. In our subsequent presentation, without causing confusion we will use notations $D_i(t)$ and $D_i(\rho)$ interchangeably where the former indicates the demand as a time-varying quantity, and the latter emphasizes demand as a function of density. The same applies to the supply.

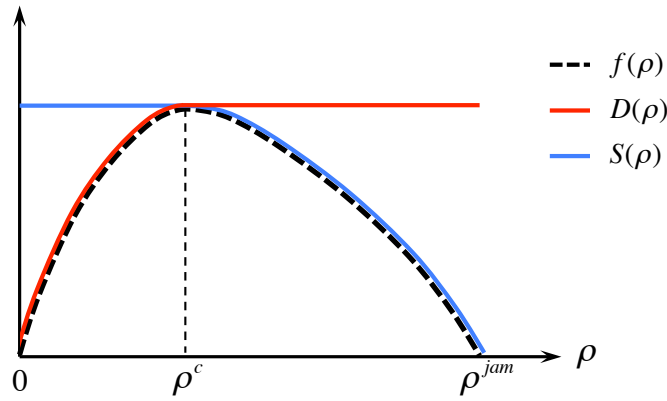


Figure 2: Demand and supply as functions of density.

3. Dynamic network loading problem formulated as a PDAE system

The aim of this section is to formulate the LWR-based dynamic network loading (DNL) problem as a system of partial differential algebraic equations (PDAEs). The proposed PDAE system uses vehicle density and queues as the primary unknown variables, and computes link dynamics, flow propagation, and path delay for any given vector of departure rates. The PDAE system captures vehicle spillback explicitly, and accommodates a wide range of junction types and Riemann Solvers.

We consider a network $G(\mathcal{A}, \mathcal{V})$ expressed as a directed graph with \mathcal{A} being the set of links and \mathcal{V} being the set of nodes. Let \mathcal{P} be the set of paths employed by travelers, and \mathcal{W} be the set of origin-destination pairs. Each path $p \in \mathcal{P}$ is expressed as an ordered set of links it traverses:

$$p = \{I_1, I_2, \dots, I_{m(p)}\}$$

where $m(p)$ is the number of links in this path. There are several crucial components of a complete network loading model, each of which is elaborated in a subsection below. Throughout the rest of this paper, for each node $v \in \mathcal{V}$, we denote by I^v the set of incoming links and O^v the set of outgoing links.

3.1. Within-link dynamics

For each $I_i \in \mathcal{A}$, the density dynamic is governed by the scalar conservation law

$$\partial_t \rho_i(t, x) + \partial_x [\rho_i(t, x) \cdot v_i(\rho_i(t, x))] = 0 \quad (t, x) \in [0, T] \times [a_i, b_i] \quad (3.8)$$

subject to initial condition and boundary conditions to be determined in Section 3.2. The fundamental diagram $f_i(\rho_i) = \rho_i \cdot v_i(\rho_i)$ satisfies condition **(F)** stated at the beginning of Section 2.2. In order to explicitly incorporate drivers' route choices, for every $p \in \mathcal{P}$ such that $I_i \in p$ we introduce the function $\mu_i^p(t, x)$, $(t, x) \in [0, T] \times [a_i, b_i]$, which represents, in every unit of flow $f_i(\rho_i(t, x))$, the fraction associated with path p . We call these variables *path disaggregation variables* (PDV). For each car moving along the link I_i , its surrounding traffic can be distinguished by path (e.g. 20% following path p_1 , 30% following path p_2 , 50% following path p_3). As this car moves, such a composition will not change since its surrounding traffic all move at the same speed under the first-in-first-out (FIFO) principle (i.e. no overtaking is allowed). In mathematical terms, this means that the path disaggregation variables, $\mu_i^p(\cdot, \cdot)$, are constants along the trajectories of cars $(t, x(t))$ in the space-time diagram, where $x(\cdot)$ is the trajectory of a moving car on link I_i . That is,

$$\frac{d}{dt} \mu_i^p(t, x(t)) = 0 \quad \forall p \text{ such that } I_i \in p,$$

which, according to the chain rule, becomes

$$\partial_t \mu_i^p(t, x(t)) + \partial_x \mu_i^p(t, x) \cdot \frac{d}{dt} x(t) = 0,$$

which further leads to another set of partial differential equations on link I_i :

$$\partial_t \mu_i^p(t, x) + v_i(\rho_i(t, x)) \cdot \partial_x \mu_i^p(t, x) = 0 \quad \forall p \text{ such that } I_i \in p \quad (3.9)$$

Here, $\rho_i(t, x)$ is the solution of (3.8). The following obvious identity holds

$$\sum_{p \ni I_i} \mu_i^p(t, x) = 1 \quad \text{whenever } \rho_i(t, x) > 0 \quad (3.10)$$

where $p \ni I_i$ means "path p contains (or traverses) link I_i ", and the summation appearing in (3.10) is with respect to all such p . By convention, if $\rho_i(t, x) = 0$, then $\mu_i^p(t, x) = 0$ for all $p \ni I_i$.

3.2. Boundary conditions at an ordinary node

For reason that will become clear later, we introduce the concept of an *ordinary node*. An ordinary node is neither the origin nor the destination of any trip. We use the notation \mathcal{V}^o to represent the set of ordinary nodes in the network.

As mentioned earlier, the partial differential equations on links incident to J are all coupled together through a given junction model, i.e., a Riemann Solver. A common prerequisite for applying the Riemann Solver is the determination of the flow distribution (turning ratio) matrix (Coclite et al., 2005), which relies on knowledge of the PDVs $\mu_i^p(t, b_i)$ for all $I_i \in \mathcal{I}^J$. We define the time-dependent flow distribution matrix associated with J :

$$A^J(t) = \{\alpha_{ij}^J(t)\} \in [0, 1]^{|I^J|+|O^J|} \quad (3.11)$$

where by convention, we use subscript i to indicate incoming links, and j to indicate outgoing links. Each element $\alpha_{ij}^J(t)$ represents the turning ratios of cars discharged from I_i that enter downstream link I_j . Then, for all p that traverses J , the following holds.

$$\alpha_{ij}^J(t) = \sum_{p \ni I_i, I_j} \mu_i^p(t, b_i) \quad \forall I_i \in \mathcal{I}^J, I_j \in \mathcal{O}^J \quad (3.12)$$

It can be easily verified that $\alpha_{ij}^J(t) \in [0, 1]$ and $\sum_j \alpha_{ij}^J(t) \equiv 1$ according to (3.10).

We are now ready to express the boundary conditions for the ordinary junction $J \in \mathcal{V}^o$. Let

$$RS^{A^J} : \prod_{k=1}^{|I^J|+|O^J|} [0, \rho_k^{jam}] \rightarrow \prod_{k=1}^{|I^J|+|O^J|} [0, \rho_k^{jam}]$$

be a given Riemann Solver. Notice that the dependence of the Riemann Solver on A^J has been indicated with a superscript. The boundary conditions for PDEs (3.8) read

$$\rho_k(t, b_k) = RS_k^{A^J} \left[(\rho_i(t, b_i^-))_{I_i \in \mathcal{I}^J}, (\rho_j(t, a_j^+))_{I_j \in \mathcal{O}^J} \right] \quad \forall I_k \in \mathcal{I}^J \quad (3.13)$$

$$\rho_l(t, a_l) = RS_l^{A^J} \left[(\rho_i(t, b_i^-))_{I_i \in \mathcal{I}^J}, (\rho_j(t, a_j^+))_{I_j \in \mathcal{O}^J} \right] \quad \forall I_l \in \mathcal{O}^J \quad (3.14)$$

where $RS_k^{A^J}[\cdot]$ denotes the k -th component of the mapping, $k = 1, \dots, |\mathcal{I}^J| + |\mathcal{O}^J|$.

Remark 3.1. Intuitively, (3.13)-(3.14) mean that, given the current traffic states $(\rho_i(t, b_i^-))_{I_i \in \mathcal{I}^J}$ and $(\rho_j(t, a_j^+))_{I_j \in \mathcal{O}^J}$ adjacent to the junction J , the Riemann Solver RS^{A^J} specifies, for each incident link I_k or I_l , the corresponding boundary conditions $\rho_k(t, b_k)$ or $\rho_l(t, a_l)$. In prose, at each time instance the Riemann Solver inspects the traffic conditions near the junction, and proposes the discharging (receiving) flows of its incoming (outgoing) links. Such a process is based on the flow distribution matrix A^J and often reflects traffic control measures at junctions. Furthermore, the Riemann Solver operates with knowledge of every link incident to the junction, thus the boundary condition of any relevant link is determined jointly by all the links connected to the same junction. Therefore, the LWR equations on all the links are coupled together through this mechanism. For this reason the LWR-based DNL models are highly challenging, both theoretically and computationally.

The upstream boundary conditions associated with PDEs (3.9) are:

$$\mu_j^p(t, a_j) = \frac{f_i(\rho_i(t, b_i)) \cdot \mu_i^p(t, b_i)}{f_j(\rho_j(t, a_j))} \quad \forall p \text{ such that } \{I_i, I_j\} \subset p, \quad \forall I_j \in \mathcal{O}^J \quad (3.15)$$

where the numerator $f_i(\rho_i(t, b_i)) \cdot \mu_i^p(t, b_i)$ expresses the exit flow on link I_i associated with path p , which, by flow conservation, is equal to the entering flow of link I_j associated with the same path p ; the denominator represents the total entering flow of link I_j .

Remark 3.2. Unlike the density-based PDE, the PDV-based PDE does not have any downstream boundary condition due to the fact that the traveling speeds of the PDVs are the same as the car speeds (they can be interpreted as Lagrangian labels that travel with the cars); thus information regarding the PDVs does not propagate backwards or spills over to upstream links.

3.3. Flow distribution at origin or destination nodes

We consider a node $v \in \mathcal{V}$ that is either the origin or the destination of some path p . One immediate observation is that the flow conservation constraint (2.4) no longer holds at such a node since vehicles either are ‘generated’ (if v is an origin) or ‘vanish’ (if v is a destination). A simple and effective way to circumvent this issue is to introduce a *virtual link*. A virtual link is an imaginary road with certain length and fundamental diagram, and serves as a buffer between an ordinary node and an origin/destination; see Figure 3 for an illustration. By introducing virtual links to the original network, we obtain an augmented network $G(\tilde{\mathcal{A}}, \tilde{\mathcal{V}})$ in which all road junctions are ordinary, and hence fall within the scope of the previous section.

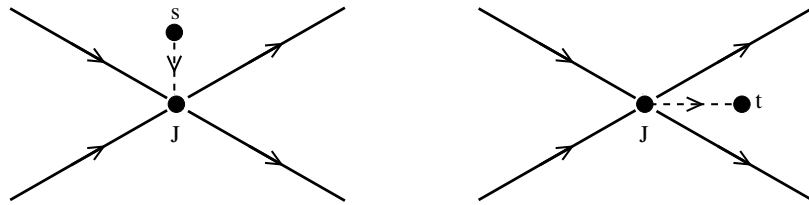


Figure 3: Illustration of the virtual links. Left: a virtual link connecting an origin (s) to an ordinary junction J . Right: a virtual link connecting a destination (t) to an ordinary junction J .

Let us denote by \mathcal{S} the set of origins in the augmented network $G(\tilde{\mathcal{A}}, \tilde{\mathcal{V}})$. For any $s \in \mathcal{S}$, we denote by $\mathcal{P}^s \subset \mathcal{P}$ the set of paths that originate from s , and by I_s the virtual link incident to this origin. For each $p \in \mathcal{P}^s$ we denote by $h_p(t)$

the departure rate (path flow) along p . It is expected that a buffer (point) queue may form at s in case the receiving capacity of the downstream I_s is insufficient to accommodate all the departure rates $\sum_{p \in \mathcal{P}^s} h_p(t)$. For this buffer queue, denoted $q_s(t)$, we employ a Vickrey-type dynamic (Vickrey, 1969); that is,

$$\frac{d}{dt}q_s(t) = \sum_{p \in \mathcal{P}^s} h_p(t) - \begin{cases} S_s(t) & \text{if } q_s(t) > 0 \\ \min \left\{ \sum_{p \in \mathcal{P}^s} h_p(t), S_s(t) \right\} & \text{if } q_s(t) = 0 \end{cases} \quad (3.16)$$

where $S_s(t)$ denotes the supply of the virtual link I_s . The only difference between (3.16) and Vickrey's model is the time-varying downstream receiving capacity provided by the virtual link.⁴

It remains to determine the dynamics for the path disaggregation variables (PDV). More precisely, we need to determine $\mu_s^p(t, a_s)$ for the virtual link I_s where $p \in \mathcal{P}^s$, and $x = a_s$ is the upstream boundary of I_s . This will be achieved using the Vickrey-type dynamic (3.16) and the FIFO principle. Specifically, we define the queue exit time function $\lambda_s(t)$ where t denotes the time at which drivers depart and join the point queue, if any; $\lambda_s(t)$ expresses the time at which the same group of drivers exit the point queue. Clearly, FIFO dictates that

$$\int_0^t \sum_{p \in \mathcal{P}^s} h_p(\tau) d\tau = \int_0^{\lambda_s(t)} f_s(\rho_s(\tau, a_s)) d\tau \quad (3.17)$$

where the two integrands on the left and right hand sides of the equation are flow entering the queue and flow leaving the queue, respectively. We may determine the path disaggregation variables as:

$$\mu_s^p(\lambda_s(t), a_s) = \frac{h_p(t)}{\sum_{q \in \mathcal{P}^s} h_q(t)} \quad \forall p \in \mathcal{P}^s \quad (3.18)$$

Notice that, if $\sum_{q \in \mathcal{P}^s} h_q(t) = 0$, then the flow leaving the point queue at time $\lambda_s(t)$ is also zero; thus there is no need to determine the path disaggregation variables. Therefore, the identity (3.18) is well defined and meaningful.

3.4. Calculation of path travel times

With all preceding discussions, we may finally express the path travel times, which are the outputs of a complete DNL model. The path travel time consists of link travel times plus possible queuing time at the origin. Mathematically, the link exit time function $\lambda_i(t)$ for any I_i is defined, in a way similar to (3.17), as

$$\int_0^t f_i(\rho_i(\tau, a_i)) d\tau = \int_0^{\lambda_i(t)} f_i(\rho_i(\tau, b_i)) d\tau \quad (3.19)$$

For a path expressed as $p = \{I_1, I_2, \dots, I_{m(p)}\}$, the time to traverse it is calculated as

$$\lambda_s \circ \lambda_1 \circ \lambda_2 \dots \circ \lambda_{m(p)}(t) \quad (3.20)$$

where $f \circ g(t) \doteq g(f(t))$ means the composition of two functions. This is due to the assumption that cars leaving the previous link (or queue) immediately enter the next link without any delay.

3.5. The PDAE system

We are now ready to present a generic PDAE system for the dynamic network loading procedure. Let us begin by summarizing some key notations.

⁴The right hand side of the ordinary differential equation (3.16) is discontinuous. An analytical treatment of this irregular equation is provided by Han et al. (2013a,b) using the variational formulation.

$G(\mathcal{A}, \mathcal{V})$	the original network with link set \mathcal{A} and node set \mathcal{V} ;
\mathcal{VL}	the set of virtual links;
$G(\tilde{\mathcal{A}}, \tilde{\mathcal{V}})$	the augmented network including virtual links;
\mathcal{S}	the set of origins in $G(\tilde{\mathcal{A}}, \tilde{\mathcal{V}})$;
\mathcal{P}^s	the set of paths originating from $s \in \mathcal{S}$;
\mathcal{V}^o	the set of ordinary junctions in $G(\tilde{\mathcal{A}}, \tilde{\mathcal{V}})$;
\mathcal{I}^J	the set of incoming links of a junction $J \in \mathcal{V}^o$;
\mathcal{O}^J	the set of outgoing links of a junction $J \in \mathcal{V}^o$;
$A^J(t)$	the flow distribution matrix associated with junction J ;
RS^{A^J}	the Riemann Solver for junction J , which depends on A^J .

We also list some key variables of the PDAE system below.

$h_p(t)$	the path departure rate along $p \in \mathcal{P}$;
$\rho_i(t, x)$	the vehicle density on link $I_i \in \tilde{\mathcal{A}}$;
$\mu_i^p(t, x)$	the proportion of flow on link I_i associated with path p (path disaggregation variable);
$q_s(t)$	the point queue at the origin $s \in \mathcal{S}$;
$\lambda_s(t)$	the point queue exit time function at origin $s \in \mathcal{S}$.

Given any vector of path departure rates $h = (h_p(\cdot) : p \in \mathcal{P})$, the proposed PDAE system for calculating path travel times is summarized as follows.

$$\frac{dq_s(t)}{dt} = \sum_{p \in \mathcal{P}^s} h_p(t) - \begin{cases} S_s(t) & q_s(t) > 0 \\ \min \left\{ \sum_{p \in \mathcal{P}^s} h_p(t), S_s(t) \right\} & q_s(t) = 0 \end{cases} \quad \forall s \in \mathcal{S} \quad (3.21)$$

$$\int_0^t \sum_{p \in \mathcal{P}^s} h_p(\tau) d\tau = \int_0^{\lambda_s(t)} f_s(\rho_s(\tau, a_s)) d\tau \quad \forall s \in \mathcal{S} \quad (3.22)$$

$$\int_0^t f_i(\rho_i(\tau, a_i)) d\tau = \int_0^{\lambda_i(t)} f_i(\rho_i(\tau, b_i)) d\tau \quad \forall I_i \in \tilde{\mathcal{A}} \quad (3.23)$$

$$\partial_t \rho_i(t, x) + \partial_x [\rho_i(t, x) \cdot v_i(\rho_i(t, x))] = 0 \quad (t, x) \in [0, T] \times [a_i, b_i] \quad (3.24)$$

$$\partial_t \mu_i^p(t, x) + v_i(\rho_i(t, x)) \cdot \partial_x \mu_i^p(t, x) = 0 \quad (t, x) \in [0, T] \times [a_i, b_i] \quad (3.25)$$

$$\mu_s^p(\lambda_s(t), a_s) = \frac{h_p(t)}{\sum_{q \in \mathcal{P}^s} h_q(t)} \quad \forall s \in \mathcal{S}, p \in \mathcal{P}_s \quad (3.26)$$

$$\mu_j^p(t, a_j) = \frac{f_i(\rho_i(t, b_i)) \cdot \mu_i^p(t, b_i)}{f_j(\rho_j(t, a_j))} \quad \forall p \supset \{I_i, I_j\} \quad (3.27)$$

$$A^J(t) = \{\alpha_{ij}^J(t)\}, \quad \alpha_{ij}^J(t) = \sum_{p \ni I_i, I_j} \mu_i^p(t, b_i) \quad \forall I_i \in \mathcal{I}^J, I_j \in \mathcal{O}^J \quad (3.28)$$

$$\rho_k(t, b_k) = RS_k^{A^J} \left[(\rho_i(t, b_i^-))_{I_i \in \mathcal{I}^J}, (\rho_j(t, a_j^+))_{I_j \in \mathcal{O}^J} \right] \quad \forall I_k \in \mathcal{I}^J \quad (3.29)$$

$$\rho_l(t, a_l) = RS_l^{A^J} \left[(\rho_i(t, b_i^-))_{I_i \in \mathcal{I}^J}, (\rho_j(t, a_j^+))_{I_j \in \mathcal{O}^J} \right] \quad \forall I_l \in \mathcal{O}^J \quad (3.30)$$

$$D_p(t, h) = \lambda_s \circ \lambda_1 \circ \lambda_2 \dots \circ \lambda_{m(p)}(t) \quad \forall p \in \mathcal{P}, \quad \forall t \in [0, T] \quad (3.31)$$

Eqn (3.21) describes the (potential) queuing process at each origin. Eqns (3.22) and (3.23) express the queue exit time function for a point queue, and the link exit time function for a link, respectively. Eqns (3.24)-(3.25) express the link dynamics in terms of car density and PDV; Eqns (3.26)-(3.27) specifies the upstream boundary conditions for the PDV as these variables can only propagate forward in space. Eqns (3.28)-(3.30) determine the boundary conditions at junctions. Finally, Eqn (3.31) determines the path travel times.

The above PDAE system involves partial differential operators ∂_t and ∂_x . Solving such a system requires solution techniques from the theory of numerical *partial differential equations* (PDE) such as finite difference methods (Godunov, 1959; LeVeque, 1992) and finite element methods (Larsson and Thomée, 2005).

4. Well-posedness of two junction models

In mathematical modeling, the term *well-posedness* refers to the property of having a unique solution, and the behavior of that solution hardly changes when there is a slight change in the initial/boundary conditions. Examples of well-posed problems include the initial value problem for scalar conservation laws (Bressan, 2000), and the initial value problem for the Hamilton-Jacobi equations (Daganzo, 2006). In the context of traffic network modeling, well-posedness is a desirable property of network performance models capable of supporting analyses and computations of DTA models. It is also closely related to the continuity of the path delay operator, which is the main focus of this paper.

This section investigates the well-posedness (i.e. continuous dependence on the initial/boundary conditions) of two specific junction models. These two junctions are depicted in Figure 4, and the corresponding merge and diverge rules are proposed initially by Daganzo (1995) in a discrete-time setting with fixed vehicle turning ratios and driving priority parameters.

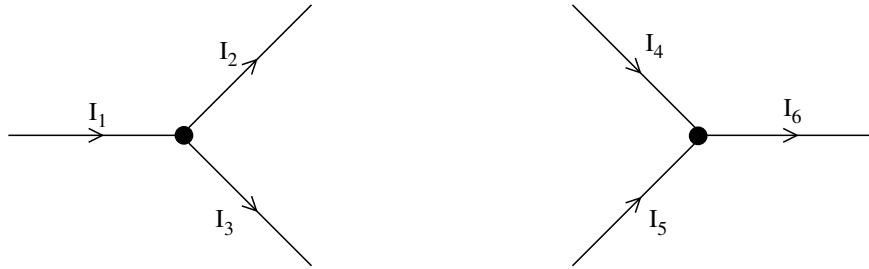


Figure 4: The diverging (left) and merge (right) junctions.

4.1. The two junction models

4.1.1. The diverge model

We first consider the diverge junction shown on the left part of Figure 4, with one incoming link I_1 and two outgoing links I_2 and I_3 . The demand $D_1(t)$ and the supplies, $S_2(t)$ and $S_3(t)$, are defined by (2.6) and (2.7) respectively. The Riemann Solver for this junction relies on the following two conditions.

(A1) Cars leaving I_1 advance to I_2 and I_3 according to some turning ratio which is determined by the PDV $\mu_1(t, b_1)$ in the DNL model.

(A2) Subject to (A1), the flow through the junction is maximized.

In the original diverge model (Daganzo, 1995), the vehicle turning ratios, denoted $\alpha_{1,2}$ and $\alpha_{1,3}$ with obvious meaning of notations, are constants known *a priori*. This is not the case in a dynamic network loading model since they are determined endogenously by drivers' route choices, as expressed mathematically by Eqn (3.28). The diverge junction model, described by (A1) and (A2), can be more explicitly written as:

$$\begin{aligned} f_1^{out}(t) &= \min \left\{ D_1(t), \frac{S_2(t)}{\alpha_{1,2}(t)}, \frac{S_3(t)}{\alpha_{1,3}(t)} \right\} \\ f_2^{in}(t) &= \alpha_{1,2}(t) \cdot f_1^{out}(t) \\ f_3^{in}(t) &= \alpha_{1,3}(t) \cdot f_1^{out}(t) \end{aligned} \quad (4.32)$$

where $f_1^{out}(t)$ denotes the exit flow of link I_1 , and $f_j^{in}(t)$ denotes the entering flow on link I_j , $j = 2, 3$.

4.1.2. The merge model

We now turn to the merge junction in Figure 4, with two incoming links I_4 and I_5 and one outgoing link I_6 . In view of this merge junction, assumption (A1) becomes irrelevant as there is only one outgoing link; and assumption (A2) cannot determine a unique solution⁵. To address this issue, we consider a *right-of-way* parameter $p \in (0, 1)$ and the following priority rule:

(R1) The actual link exit flows satisfy $(1 - p) \cdot f_4^{out}(t) = p \cdot f_5^{out}(t)$.

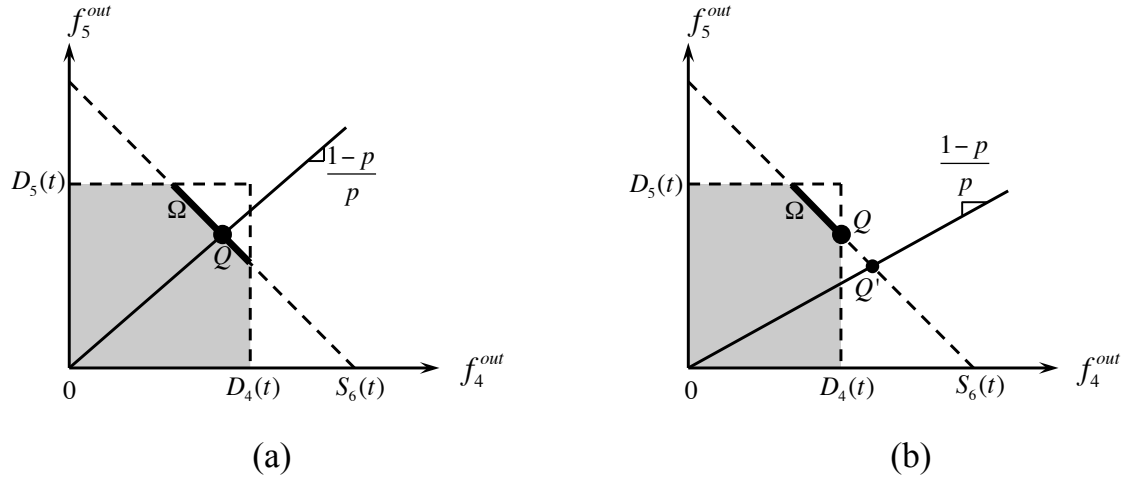


Figure 5: Illustration of the merge model. The shaded areas represent the feasible domain of the maximization problem (4.33), and the thick line segments (Ω) are the optimal solution sets of (4.33). Left: Rule (R1) is compatible with (A2); and there exists a unique point Q satisfying both (A2) and (R1). Right: (R1) is incompatible with (A2); in this case, the model selects point Q within the set Ω that is closest to the ray (R) from the origin with slope $\frac{1-p}{p}$.

Notice that (R1) may be incompatible with assumption (A2); and we refer the reader to Figure 5 for an illustration. Whenever there is a conflict between (R1) and (A2), we always respect (A2) and relax (R1) so that the solution is chosen to be the point that is closest to the line $y = \frac{1-p}{p}x$ among all the points yielding the maximum flow. Clearly, such a point is unique. Mathematically, we let Ω be the set of points (f_4^{out}, f_5^{out}) that solves the following maximization problem:

$$\begin{cases} \max f_4^{out} + f_5^{out} \\ \text{such that } 0 \leq f_4^{out} \leq D_4(t), 0 \leq f_5^{out} \leq D_5(t), f_4^{out} + f_5^{out} \leq S_6(t) \end{cases} \quad (4.33)$$

Moreover, we define the ray $R \doteq \{(f_4^{out}, f_5^{out}) \in \mathbb{R}_+^2 : (1 - p) \cdot f_4^{out} = p \cdot f_5^{out}\}$. Then the solution of the merge model is defined to be the projection of R onto Ω ; that is,

$$(f_4^{out,*}, f_5^{out,*}) = \underset{(f_4^{out}, f_5^{out}) \in \Omega}{\operatorname{argmin}} d[(f_4^{out}, f_5^{out}), R] \quad (4.34)$$

where $d[(f_4^{out}, f_5^{out}), R]$ denotes the Euclidean distance between the point (f_4^{out}, f_5^{out}) and the ray R :

$$d[(f_4^{out}, f_5^{out}), R] = \min_{(x,y) \in R} \|(f_4^{out}, f_5^{out}) - (x, y)\|_2$$

⁵More generally, as pointed out by Coclite et al. (2005), when the number of incoming links exceeds the number of outgoing links, (A1) and (A2) combined are not sufficient to ensure a unique solution.

4.2. Well-posedness of the diverge junction model

In this section, we investigate the well-posedness of the diverge junction model. Unlike previous studies (Garavello and Piccoli, 2006; Han et al., 2015b), a major challenge in this case is to incorporate drivers' route choices, expressed by the *path disaggregation variable* μ , into the model and the analysis. In effect, we need to establish the continuous dependence of the model on the initial/boundary conditions in terms of both ρ and μ . As we shall see in Section 4.2.1 below, such a continuity does not hold in general. Following this, Section 4.2.2 provides sufficient conditions for the continuity to hold. These sufficient conditions are crucial for the desired continuity of the delay operator.

4.2.1. An example of ill-posedness

It has been shown by Han et al. (2015b) that the diverge model (Section 4.1.1) with constant turning ratios, $\alpha_{1,2}$ and $\alpha_{1,3}$, is well-posed. However, the assumption of fixed and exogenous turning ratios does not hold in DNL models; see (3.28). As a result the well-posedness is no longer true, which is demonstrated by the following counterexample.

We consider the diverge junction (Figure 4) and assume the same fundamental diagram $f(\cdot)$ for all the links for simplicity. We consider a series of constant initial data parameterized by ε on the three links I_1 , I_2 , and I_3 :

$$\rho_1(0, x) \equiv \hat{\rho}_1 \in (\rho^c, \rho^{jam}), \quad \rho_2(0, x) \equiv \hat{\rho}_2^\varepsilon \in (\rho^c, \rho^{jam}], \quad \rho_3(0, x) \equiv \hat{\rho}_3^\varepsilon \in (0, \rho^c) \quad (4.35)$$

where ρ^c and ρ^{jam} are the critical density and the jam density, respectively. $\hat{\rho}_1$, $\hat{\rho}_2^\varepsilon$, and $\hat{\rho}_3^\varepsilon$ satisfy:

$$f(\hat{\rho}_2^\varepsilon) = \varepsilon f(\hat{\rho}_1), \quad f(\hat{\rho}_3^\varepsilon) = (1 - \varepsilon) f(\hat{\rho}_1) \quad (4.36)$$

where $\varepsilon \geq 0$ is a parameter. This configuration of initial data implies that link I_1 and link I_2 are both in the congested phase, while link 3 is in the uncongested (free-flow) phase, see Figure 6 for an illustration.

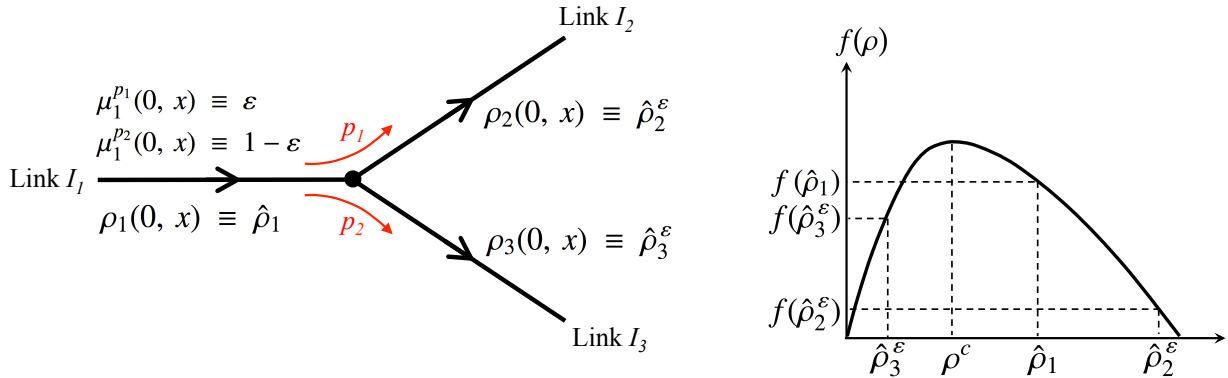


Figure 6: An example of ill-posedness of the initial value problem with endogenous route choices. Left: junction topology. Right: illustration of the constant initial densities on the links.

Two paths exist in this example: $p_1 = \{I_1, I_2\}$ and $p_2 = \{I_1, I_3\}$. The initial conditions for $\mu_1^{p_1}$ and $\mu_1^{p_2}$, which arise from travelers' route choices, are as follows.

$$\mu_1^{p_1}(0, x) \equiv \varepsilon, \quad \mu_1^{p_2}(0, x) \equiv 1 - \varepsilon$$

Notice that these initial conditions are part of the initial value problem at the junction. The solution of this initial value problem depends on the value of ε ; in particular, we have the following two cases.

- When $\varepsilon > 0$, we claim that the initial conditions $\hat{\rho}_1$, $\hat{\rho}_2^\varepsilon$ and $\hat{\rho}_3^\varepsilon$ satisfying (4.35)-(4.36) constitute a constant solution at the junction. To see this, we follow the junction model (4.32) and the definitions of demand and supply (2.6)-(2.7) to get

$$f_1^{out}(t) = \min \left\{ D_1(t), \frac{S_2(t)}{\alpha_{1,2}}, \frac{S_3(t)}{\alpha_{1,3}} \right\} = \min \left\{ C, \frac{f(\hat{\rho}_2^\varepsilon)}{\varepsilon}, \frac{C}{1 - \varepsilon} \right\} = \min \left\{ C, f(\hat{\rho}_1), \frac{C}{1 - \varepsilon} \right\} = f(\hat{\rho}_1) \quad (4.37)$$

$$f_2^{in}(t) = \alpha_{1,2} \cdot f_1^{out}(t) = \varepsilon f(\hat{\rho}_1) = f(\hat{\rho}_2^\varepsilon) \quad (4.38)$$

$$f_3^{in}(t) = \alpha_{1,3} \cdot f_1^{out}(t) = (1 - \varepsilon) f(\hat{\rho}_1) = f(\hat{\rho}_3^\varepsilon) \quad (4.39)$$

where C denotes the flow capacity. Thus $\hat{\rho}_1, \hat{\rho}_2^\varepsilon$ and $\hat{\rho}_3^\varepsilon$ form a constant solution at the junction.

- When $\varepsilon = 0$, the turning ratios satisfy $\alpha_{1,2}(t) \equiv 0, \alpha_{1,3}(t) \equiv 1$. Effectively, link I_1 is only connected to link I_3 . We easily deduce that

$$f_1^{out}(t) \equiv C \quad (4.40)$$

$$f_2^{in}(t) \equiv 0 \quad (4.41)$$

$$f_3^{in}(t) \equiv C \quad (4.42)$$

As a result, the solution on link I_1 is given by a backward-propagating rarefaction wave (or expansion wave, fan wave) with $\hat{\rho}_1$ and ρ^c on the two sides. On link I_3 , a forward-propagating rarefaction wave with ρ^c and $\hat{\rho}_3^0$ (that is, the limit of $\hat{\rho}_3^\varepsilon$ as $\varepsilon \rightarrow 0$) on the two sides is created. Link I_2 remains in a completely jam state with full density ρ^{jam} . See Figure 7 for an illustration of the solutions.

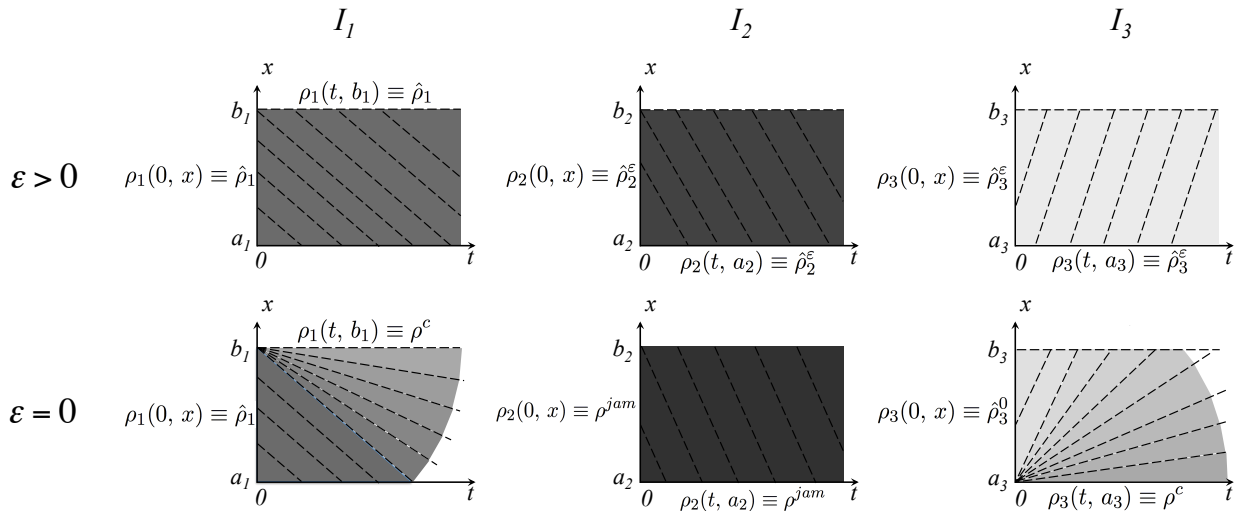


Figure 7: Comparison of solutions on I_1, I_2 and I_3 for the two cases: $\varepsilon > 0$ and $\varepsilon = 0$. The dashed lines represent the kinematic waves (characteristics), and darker color indicates higher density. Notice that jumps in the boundary conditions across these two cases exist on I_1 and I_3 .

The two sets of solutions corresponding to $\varepsilon > 0$ and $\varepsilon = 0$ are shown in Figure 7. We first notice that in these two cases, the boundary flows are very different, despite the infinitesimal difference in the PDV, namely from $\varepsilon > 0$ to $\varepsilon = 0$. In particular, both $f_1^{out}(t)$ and $f_3^{in}(t)$ jump from $f(\hat{\rho}_1)$ and $f(\hat{\rho}_3^\varepsilon)$ (when $\varepsilon > 0$) to C (when $\varepsilon = 0$). This is a clear indication of the discontinuous dependence of the diverge junction model on its initial conditions.

Let us zoom in on the mechanism that triggers such a discontinuity. According to (4.37), the expression for $f_1^{out}(t)$ when $\varepsilon > 0$ is

$$f_1^{out}(t) = \min \left\{ C, \frac{f(\hat{\rho}_2^\varepsilon)}{\varepsilon}, \frac{C}{1-\varepsilon} \right\} = \min \left\{ C, \frac{\varepsilon f(\hat{\rho}_1)}{\varepsilon} \right\}$$

As long as ε is positive, the fraction $\frac{\varepsilon f(\hat{\rho}_1)}{\varepsilon} = f(\hat{\rho}_1) < C$. However, when $\varepsilon = 0$ we have an expression of $\frac{0}{0}$, which should be equal to ∞ since link I_2 has effectively no influence on the junction, and we have $\min\{C, \frac{0}{0}\} = C$. The above argument amounts to the following statement:

$$\begin{aligned} \text{if } \varepsilon > 0, & \quad C > \frac{\varepsilon f(\hat{\rho}_1)}{\varepsilon}; \\ \text{if } \varepsilon = 0, & \quad C < \frac{\varepsilon f(\hat{\rho}_1)}{\varepsilon}, \end{aligned}$$

which explains the jump in the solutions when ε tends to zero.

Remark 4.1. *The fact that $\hat{\rho}_2^\varepsilon$ tends to ρ^{jam} as $\varepsilon \rightarrow 0$ plays a key role in this example. As we shall see later in Theorem 4.2, bounding $\hat{\rho}_2^\varepsilon$ away from the jam density is essential for the well-posedness.*

4.2.2. Sufficient conditions for the well-posedness of the diverge model

As we have previously demonstrated, the diverge model with time-varying vehicle turning ratios may not depend continuously on its initial conditions, which are defined in terms of the two-tuple (ρ, μ) . In this section, we propose additional conditions that guarantee the continuous dependence with respect to the initial data at the diverge junction. Our analysis relies on the method of wave-front tracking (Bressan, 2000; Garavello and Piccoli, 2006) and the technique of *generalized tangent vectors* (Bressan, 1993; Bressan et al., 2000). In order to be self-contained while keeping our presentation concise, we move some general background on these subjects and essential mathematical details to Appendix A.

Theorem 4.2. (Well-posedness of the diverge model) *Consider the diverge junction (Figure 4) and assume that*

1. *there exists some $\delta > 0$ such that the supplies $S_2(t) \geq \delta$, $S_3(t) \geq \delta$ for all t ;*
2. *the path disaggregation variable $\mu(t, x)$ has bounded total variation in t .*

Then the solution of the diverge junction depends continuously on the initial and boundary conditions in terms of ρ and μ .

Proof. The proof is long and technical, and thus will be presented in Appendix B.1 following necessary mathematical preliminaries in Appendix A. □

4.3. Well-posedness of the merge model

For the merge junction depicted in Figure 4, the path disaggregation variables μ become irrelevant since there is only one downstream link. According to Theorem 5.3 of Han et al. (2015b), the solution at the merge junction, in terms of density ρ , depends continuously on the initial and boundary conditions. Moreover, according to (3.9), the propagation speed of μ is the same as the vehicle speed $v(\rho)$, we thus conclude that μ also depends continuously on the initial and boundary conditions. This shows the well-posedness of the merge junction.

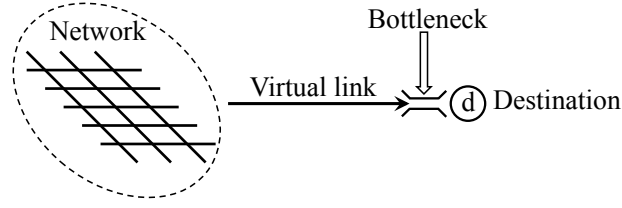
5. Continuity of the delay operator

The proof of the continuity of the path delay operator is outlined as follows. We first show that the first hypothesis of Theorem 4.2 holds for networks that consists of only the merge and diverge junctions discussed in Section 4.1; this will be done in Section 5.1. Then, we propose some mild conditions on the fundamental diagram and the departure rates in Section 5.2 to ensure that the second hypothesis of Theorem 4.2 holds. It then follows that both the merge and diverge models are well posed. Finally, in Section 5.3 we show the well-posedness of the model in terms of ρ and μ at each origin, where a point queue may be present. Put altogether, these results lead to the desired continuity for the delay operator.

5.1. An estimation of minimum network supply

This section provides a lower bound on the supply, which is a function of density, on any link in the network during the entire time horizon $[0, T]$. Our finding is that the jam density can never be reached within any finite time horizon T , and the supply anywhere in the network is bounded away from zero. As a consequence, grid lock will never occur in the dynamic network.

We denote by \mathcal{D} the set of destinations in the augmented network with virtual links (see Section 3.3); that is, every destination $d \in \mathcal{D}$ is incident to a virtual link that connects d to the rest of the network; see Figure 8. For each $d \in \mathcal{D}$, we introduce its supply, denoted S^d , to be the maximum rate at which cars can be discharged from the virtual link connected to d . Effectively, there exists a bottleneck between the virtual link and the destination; and the supply of the destination is equal to the flow capacity of this bottleneck; see Figure 8. Notice that in some literature such a bottleneck is completely ignored and the destination is simply treated as a sink with infinite receiving capacity. This is of course a special case of ours once we set the supply S^d to be infinity. However, such a supply may be finite and

Figure 8: Illustration of the supply (receiving capacity) of the destination d .

even quite limited under some circumstances due to, for example, ramp metering, limited parking spaces, or the fact that the destination is an aggregated subnetwork that is congested.

We introduce below a few more concepts and notations.

$L = \min_{I_i \in \bar{\mathcal{A}}} L_i$: the minimum link length in the network, including virtual links.

$C^{min} = \min_{I_i \in \bar{\mathcal{A}}} C_i$: the minimum link flow capacity in the network, including virtual links.

$\lambda = \max_{I_i \in \bar{\mathcal{A}}} |f'_i(\rho_i^{jam})|$: the maximum backward wave speed in the network.

$\bar{p} = \min_{J \in \mathcal{V}_M} \{p^J, 1 - p^J\} > 0$, where p^J is the priority parameter for the merge junction J (see Section 4.1.2), \mathcal{V}_M denotes the set of merge junctions in the network.

$\delta^{\mathcal{D}} = \min_{d \in \mathcal{D}} S^d > 0$: the minimum supply among all the destination nodes.

$\delta_k = \min_{I_i \in \bar{\mathcal{A}}} \inf_{t \in [k\frac{L}{\lambda}, (k+1)\frac{L}{\lambda}]} \inf_{x \in [a_i, b_i]} S_i(\rho_i(t, x))$: the minimum supply at any location in the network during time interval $[k\frac{L}{\lambda}, (k+1)\frac{L}{\lambda}]$, where $k = 0, 1, \dots$

Theorem 5.1. Consider a network consisting of only merge and diverge junctions as shown in Figure 4. Given any vector of path departure rates, the dynamic network loading procedure described by the PDAE system yields the following property in the solution:

$$\delta_k \geq \bar{p}^k \min \{ \delta^{\mathcal{D}}, \bar{p} C^{min} \} \quad \forall k = 0, 1, \dots \quad (5.43)$$

Proof. We postpone the proof until Appendix B.2 for a more compact presentation. \square

Theorem 5.1 guarantees that the supply values anywhere in the network during the period $[k\frac{L}{\lambda}, (k+1)\frac{L}{\lambda}]$ are uniformly bounded below by some constant that depends only on k , although such a constant may decay exponentially as k increases. Given that any dynamic network loading problem is conceived in a finite time horizon, we immediately obtain a lower bound on the supplies, as shown in the corollary below.

Corollary 5.2. Under the same setup as Theorem 5.1, we have

$$\min_{I_i \in \bar{\mathcal{A}}} \inf_{x \in [a_i, b_i]} S_i(\rho_i(t, x)) \geq \bar{p}^{\lfloor \frac{t}{L/\lambda} \rfloor} \{ \delta^{\mathcal{D}}, \bar{p} C^{min} \} \quad \forall t \in [0, T] \quad (5.44)$$

and

$$\min_{I_i \in \bar{\mathcal{A}}} \inf_{x \in [a_i, b_i]} \inf_{t \in [0, T]} S_i(\rho_i(t, x)) \geq \bar{p}^{\lfloor \frac{T}{L/\lambda} \rfloor} \min \{ \delta^{\mathcal{D}}, \bar{p} C^{min} \} \quad (5.45)$$

where the operator $\lfloor \cdot \rfloor$ rounds its argument to the nearest integer from below.

Proof. Both inequalities are immediately consequences of (5.43). \square

Remark 5.3. *Corollary 5.2 shows that, for any network consisting of the merge and diverge junctions, the supply values are uniformly bounded from below at any point in the spatial-temporal domain. In particular, a jam density can never occur. Moreover, such a network is free of complete gridlock⁶.*

5.2. Estimation regarding the path disaggregation variables

In this section we establish some properties of the path disaggregation variable μ , which serve to validate the second hypothesis of Theorem 4.2.

Lemma 5.4. *Assume that there exists $M > 0$ and $\epsilon > 0$ so that the following hold:*

1. *For all links I_i , the fundamental diagrams $f_i(\cdot)$ are uniformly linear near the zero density; more precisely, $f'_i(\rho)$ is constant for $\rho \in [0, \epsilon]$ for all $I_i \in \tilde{\mathcal{A}}$.*
2. *Each $f_i(\cdot)$ has non-vanishing derivative, i.e. $|f'_i(\rho)| \geq \epsilon, \forall \rho \in [0, \rho_i^{jam}]$.*
3. *The departure rates $\{h_p(\cdot), p \in \mathcal{P}\}$ are uniformly bounded, have bounded total variation (TV), and bounded away from zero when they are non-zero; i.e. $TV(h_p) < M$ and $h_p(t) \in \{0\} \cup [\epsilon, M]$ for all $p \in \mathcal{P}$ and almost every $t \in [0, T]$.*

Then the path disaggregation variables $\mu(t, x)$ are either zero, or uniformly bounded away from zero. Moreover, they have bounded variation.

Proof. The proof is moved to Appendix B.3. \square

Remark 5.5. *Notice that assumptions 1 and 2 of Lemma 5.4 are satisfied by the Newell-Daganzo (triangular) fundamental diagrams, where both the free-flow and congested branches of the FD are linear. Moreover, given an arbitrary fundamental diagram, one can always make minimum modifications at $\rho = 0$ and $\rho = \rho^c$ to comply with conditions 1 and 2. Assumption 3 of Lemma 5.4 is satisfied by any departure rate that is a result of a finite number of cars entering the network. And, again, any departure rate can be adjusted to satisfy this condition with minor modifications.*

5.3. Well-posedness of the queuing model at the origin with respect to departure rates

In this section we discuss the continuous dependence of the queues $q_s(t)$ and the solutions ρ_i and μ_i^p with respect to the path departure rates $h_p(t)$, $p \in \mathcal{P}$. The analysis below relies on knowledge of the wave-front tracking algorithm and generalized tangent vector, for which an introduction is provided in Appendix A.

Following Herty et al. (2007), we introduce a generalized tangent vector $(\eta_s, \xi_\rho^i, \xi_\mu^{i,p})$ for the triplet (q_s, ρ_i, μ_i^p) where $\eta_s \in \mathbb{R}$ is a scalar shift of the queue $q_s(\cdot)$, i.e. the shifted queue is $q_s(\cdot) + \eta_s$, while the tangent vectors of ρ_i and μ_i^p are defined in the same way as in Appendix A.2. The tangent vector norm of η_s is simply its absolute value $|\eta_s|$.

Lemma 5.6. *Assume that the departure rates $\{h_p(\cdot), p \in \mathcal{P}\}$ are piecewise constant, and let ξ_p be a tangent vector defined via shifting the jumps in $h_p(\cdot)$. Then the tangent vector $(\eta_s, \xi_\rho^i, \xi_\mu^{i,p})$ is well defined, and its norm is equal to that of ξ_p and bounded for all times.*

Proof. The proof is postponed until Appendix B.4. \square

⁶A complete gridlock refers to the situations where a non-zero static solution of the PDAE system exists. Intuitively, it means that a complete jam $\rho = \rho^{jam}$ is formed somewhere in the network and the static queues do not dissipate in finite time.

5.4. Final proof of continuity for the delay operator

At the end of this paper, we are able to prove the continuity result for the delay operator based on a series of preliminary results presented so far.

Theorem 5.7. (Continuity of the delay operator) *Consider a network consisting of merge and diverge junctions described in Section 4.1, under the same assumptions stated in Lemma 5.4, the path delay operator, as a result of the dynamic network loading model (3.21)-(3.31), is continuous.*

Proof. We have shown that at each node (origin, diverge node, or merge node), the solution depends continuously on the initial and boundary values. In addition, between any two distinct nodes, the propagation speeds of either ρ -waves or μ -waves are uniformly bounded. Thus such well-posedness continues to hold on the network level. Consequently, the vehicle travel speed $v_i(\rho_i)$ for any I_i depends also continuously on the departure rates. We thus conclude that the path travel times depend continuously on the departure rates. \square

The assumption that the network consists of only merge and diverge nodes is not restrictive since junctions with general topology can be decomposed into a set of elementary junctions of the merge and diverge type (Daganzo, 1995). In addition, junctions that are also origins/destinations can be treated in a similar way by introducing virtual links.

Here, we would like to comment on the assumptions made in the proof of the continuity. In a recent paper (Bressan and Yu, 2015), a counterexample of uniqueness and continuous dependence of solutions is provided under certain conditions. More precisely, the authors construct the counterexample by assuming that the path disaggregation variables μ_i^p have infinite total variation. This shows the necessity of the second assumption of Theorem 4.2. Moreover, again in Bressan and Yu (2015), the authors prove that for density oscillating near zero the solution may not be unique (even in the case of bounded total variation), which shows the necessity of the third assumption in Lemma 5.4.

Remark 5.8. *Szeto (2003) provides an example of discontinuous dependence of the path travel times on the path departure rates using the cell transmission model representation of a signal-controlled network. In particular, the author showed that when a queue generated by the red signal spills back into the upstream junction, the experienced path travel time jumps from one value to another. This, however, does not contradict our result presented here for the following reason: the jam density caused by the red signal in Szeto (2003) does not exist in our network, which has only merge and diverge junctions (without any signal controls). Indeed, as shown in Corollary 5.2, the supply functions at any location in the network are uniformly bounded below by a positive constant, and thus the jam density never occurs in a finite time horizon.*

The reader is reminded of the example presented in Section 4.2.1, where the ill-posedness of the diverge model is caused precisely by the presence of a jam density. The counterexample from Szeto (2003) is constructed essentially in the same way as our example, by using signal controls that create the jam density.

We offer some further insights here on the extension of the continuity result to second-order traffic flow models. To the best of our knowledge, second-order models on traffic networks are mainly based on the Aw-Rascle-Zhang model (Garavello and Piccoli, 2006; Haut and Bastin, 2007; Herty and Rascle, 2006) and the phase-transition model (Colombo et al., 2010). Solutions of the Aw-Rascle-Zhang system may present the vacuum state, which, in general, may prevent continuous dependence (Godvik and Hanche-Olsen, 2008). On the other hand, the phase transition model on networks behaves in a way similar to the LWR scalar conservation law model. However, continuous dependence may be violated for density close to maximal; see Colombo et al. (2010). Therefore, extensions of the continuity result to second-order models appear possible only for the phase-transition type models with appropriate assumptions on the maximal density achievable on the network, but this is beyond the scope of this paper.

6. Conclusion

This paper presents, for the first time, a rigorous continuity result for the path delay operator based on the LWR network model with spillback explicitly captured. This continuity result is crucial to many dynamic traffic assignment models in terms of solution existence and computation. Similar continuity results have been established in a number of studies, all of which are concerned with non-physical queue models. As we show in Section 4.2.1, the well-posedness

of a diverge model may not hold when spillback occurs. This observation, along with others made in previous studies (Szeto, 2003), have been the major source of difficulty in showing continuity of the delay operator. In this paper, we bridge this gap through rigorous mathematical analysis involving the wave front tracking method and the generalized tangent vectors. In particular, by virtue of the finite propagation speeds of ρ -waves and μ -waves, the continuity of the delay operator boils down to the well-posedness of nodal models, including models for the origins, diverge nodes, and merge nodes. Minor assumptions are made on the fundamental diagram and the path departure rates in order to provide an upper bound on the total variations of the density ρ and the path disaggregation variables μ , which subsequently leads to the desired well-posedness of the nodal models and eventually the continuity of the operator.

A crucial step of the above process is to estimate and bound from below the minimum network supply, which is defined in terms of local vehicle densities. In fact, if the supply of some link tends to zero, the well-posedness of the diverge junction may fail as we demonstrate in Section 4.2.1. This has also been confirmed by an earlier study (Szeto, 2003), where a wave of jam density is triggered by a signal red light and causes spillback at the upstream junction, leading to a jump in the path travel times. Remarkably, in this paper we are able to show that (1) if the supply is bounded away from zero, then the diverge junction model is well posed; and (2) the desired boundedness of the supply is a natural consequence of the dynamic network loading procedure that involves only the simple merge and diverge junction models. This is a highly non trivial result because it not only plays a role in the continuity proof, but also implies that gridlock can never occur in the network loading procedure in a finite time horizon. However, we note that in numerical computations gridlock may very well occur due to finite approximations and numerical errors, while our no-gridlock result is conceived in a continuous-time and analytical (i.e., non-numerical) framework.

It is true that, despite the correctness of our result regarding the lower bound on the supply, zero supply (or gridlock) can indeed occur in real-life traffic networks as a result of signal controls. In fact, this is how Szeto (2003) constructs the counter example of discontinuity. Nevertheless, signal control is an undesirable feature of the dynamic network loading model for far more obvious reasons: the on-and-off signal control creates a lot of jump discontinuities in the travel time functions, making the existence of dynamic user equilibria (DUE) almost impossible. Given that the main purpose of this paper is to address fundamental modeling problems pertinent to DUEs, it is quite reasonable for us to avoid junction models that explicitly involve the on-and-off signal controls. Nevertheless, there exist a number of ways in which the on-and-off signal control can be approximated using continuum (homogenization) approaches. Some examples are given in Aboudolas et al. (2009); Gazis and Potts (1963); Han et al. (2014) and Han and Gayah (2015).

Regarding the exponential decay of the minimum supply, we point out that, as long as the jam density (gridlock) does not occur, our result is still applicable. From a practical point of view most networks reach congestion during day time but are almost empty during night time. In other words, the asymptotic gridlock condition is never reached in reality. Therefore, we think that our result is a reasonable approximation of reality for DUE problems.

We would also like to comment on the continuity result for other types of junction models. Garavello and Piccoli (2006) prove that Lipschitz continuous dependence on the initial conditions may fail in the presence of junctions with at least two incoming and two outgoing roads. Notably, the counterexample that they use to disprove the Lipschitz continuity is valid even when the turning ratio matrix A^J is constant and not dependent on the path disaggregation variables μ_i^p . It is interesting to note that, in the same book, continuity results for general networks are provided, but only for Riemann Solvers at junctions that allow re-directing traveling entities – a feature not allowed in the dynamic network loading model but instead is intended for the modeling of data networks.

The findings made in this paper has the following important impacts on DTA modeling and computation. (1) The analytical framework proposed for proving or disproving the well-posedness of junction models and the continuity property can be applied to other junction types and Riemann Solvers, leading to a set of continuity/discontinuity results of the delay operators for a variety of networks. (2) The established continuity result not only guarantees the existence and computation of continuous-time DUEs based on the LWR model, but also sheds light on discrete-time DUE models and provides useful insights on the numerical computations of DUEs. In particular, the various findings made in this paper provide valuable guidance on numerical procedures for the DNL problem based on the cell transmission model (Daganzo, 1994, 1995), the link transmission model (Yperman et al., 2005), or the kinematic wave model (Han et al., 2015b; Lu et al., 2013), such that the resulting delay operator is continuous on finite-dimensional spaces. As a result, the existence and computation of discrete-time DUEs will also benefit from this research.

Appendix A. Essential mathematical background

Appendix A.1. Wave-front tracking method

The wave-front tracking (WFT) method was originally proposed by Dafermos (1972) as an approximation scheme for the following initial value problem

$$\begin{cases} \partial_t \rho(t, x) + \partial_x f(\rho(t, x)) = 0 \\ \rho(0, x) = \hat{\rho}(x) \end{cases} \quad (\text{A.1})$$

where the initial condition $\hat{\rho}(\cdot)$ is assumed to have *bounded variation* (BV) (Bressan, 2000). The WFT approximates the initial condition $\hat{\rho}(\cdot)$ using *piecewise constant* (PWC) functions, and approximates $f(\cdot)$ using *piecewise affine* (PWA) functions. It is an event-based algorithm that resolves a series of wave interactions, each expressed as a Riemann Problem (RP). The WFT method is primarily used for showing existence of weak solutions of conservation laws by successive refinement of the initial data and the fundamental diagram; see Bressan (2000) and Holden and Risebro (1995). Garavello and Piccoli (2006) extend the WFT to treat the network case and show the existence of the weak solution on a network. We provide a brief description of this procedure below.

Fix a Riemann Solver (RS) for each road junction in the network. Consider a family of piecewise constant approximations $\hat{\rho}_i^\varepsilon(x)$ of the initial condition $\hat{\rho}_i(x)$ on each link and a family of piecewise affine approximation of the fundamental diagrams $f_i^\varepsilon(\rho)$, where ε is a parameter such that $\hat{\rho}_i^\varepsilon(x) \rightarrow \hat{\rho}_i(x)$ and $f_i^\varepsilon(\rho) \rightarrow f_i(\rho)$ as $\varepsilon \rightarrow 0$. A WFT approximate solution on the network is constructed as follows.

1. Within each link, solve a Riemann Problem at each discontinuity of the PWC initial data. At each junction, solve a Riemann Problem with the given RS.
2. Construct the solution by gluing together the solutions of individual RPs up to the first time when two traveling waves interact, or when a wave interacts with a junction.
3. For each interaction, solve a new RP and prolong the solution up to the next time of any interaction.
4. Repeat the processes 2 - 3.

To show that the procedure described above indeed produces a well-defined approximate solution on the network, one needs to ensure that the following three quantities are bounded: (1) the total number of waves; (2) the total number of interactions (including wave-wave and wave-junction interactions); and (3) the *total variation* (TV) of the piecewise constant solution at any point in time. These quantities are known to be bounded in the single conservation law case; in fact, they all decrease in time (Bressan, 2000). However, for the network case, one needs to proceed carefully in estimating these quantities as they may increase as a result of a wave interacting with a junction, which may produce new waves in all other links incident to the same junction. The reader is referred to Garavello and Piccoli (2006) for more elaborated discussion on these interactions. For a sequence of approximate WFT solutions ρ^ε , $\varepsilon > 0$, if one can show that the total variation of ρ^ε is uniformly bounded, then as $\varepsilon \rightarrow 0$ a weak entropy solution on the network is obtained.

Appendix A.2. Generalized tangent vector

The generalized tangent vector is a technique proposed by Bressan (1993) to show the well-posedness of conservation laws, and is used later by Garavello and Piccoli (2006) to show the well-posedness of junction models in connection with the LWR model. Its mathematical contents are briefly recapped here.

Given a piecewise constant function $F(x) : [a, b] \rightarrow \mathbb{R}$, a *tangent vector* is defined in terms of the shifts of the discontinuities of $F(\cdot)$. More precisely, let us indicate by $\{x_k\}_{k=1}^N$ the discontinuities of F where $a = x_0 < x_1 < \dots < x_N < x_{N+1} = b$, and by $\{F_k\}_{k=1}^{N+1}$ the values of F on (x_{k-1}, x_k) . A tangent vector of $F(\cdot)$ is a vector $\xi = (\xi_1, \dots, \xi_N) \in \mathbb{R}^N$ such that for each $\varepsilon > 0$, one may define the corresponding perturbation of $F(\cdot)$, denoted by $F^\varepsilon(\cdot)$ and given by

$$F^\varepsilon(x) = F_k \quad x \in [x_{k-1} + \varepsilon\xi_{k-1}, x_k + \varepsilon\xi_k)$$

for $k = 1, \dots, N + 1$, where we set $\xi_0 = \xi_{N+1} = 0$. The norm of the tangent vector ξ is defined as

$$\|\xi\| \doteq \sum_{k=1}^N |\xi_k| \cdot |F(x_{k+}) - F(x_{k-})| \quad (\text{A.2})$$

In other words, the norm of the tangent vector is the sum of each $|\xi_k|$ multiplied by the magnitude of the shifted jumps.

The procedure of showing the well-posedness of a junction model using the tangent vectors is as follows. Given piecewise constant initial/boundary conditions on each link incident to the junction, one considers their tangent vectors. By showing that the norms of their tangent vectors are uniformly bounded in time among all approximate wave-front tracking solutions, it is guaranteed that the L^1 distance of any two solutions is bounded, up to a multiplicative constant, by the L^1 distance of their respective initial/boundary conditions. More precisely, we have the following theorem

Theorem Appendix A.1. *If the norm of a tangent vector at any time is bounded by the product of its initial norm and a positive constant, among all approximate wave-front tracking solutions, then the junction model is well posed and has a unique solution.*

Proof. See Garavello and Piccoli (2006). □

Throughout this paper, we employ the notation (ρ_i, ρ_i^-) to represent a wave interacting with the junction from road I_i , where ρ_i^- is the density value in front of the wave (in the same direction as the traveling wave) and ρ_i is the density behind the wave. After the interaction, a new wave may be created on some road I_j (it is possible that $I_j = I_i$), and we use ρ_j^- and ρ_j^+ to denote the density at J on road I_j before and after the interaction, respectively.

Lemma Appendix A.2. *Consider the diverge model in Section 4.1.1. If a wave (ρ_i, ρ_i^-) on I_i interacts with J then the shift ξ_j produced on any I_j , as a result of the shift ξ_i on I_i , satisfies*

$$\xi_j(\rho_j^+ - \rho_j^-) = \frac{\Delta q_j}{\Delta q_i} \xi_i(\rho_i^+ - \rho_i^-) \quad (\text{A.3})$$

where

$$\Delta q_i \doteq f_i(\rho_i^+) - f_i(\rho_i^-), \quad \Delta q_j \doteq f_j(\rho_j^+) - f_j(\rho_j^-)$$

are the jumps in flow across these two waves.

Proof. To fix the ideas, we assume that I_i is the incoming road I_1 (the other cases can be treated in a similar way). Let (ρ_1, ρ_1^-) be the interacting wave, then it must be that $\rho_1 \leq \sigma$.

If no wave is reflected on road I_1 after the interaction (i.e. no new backward wave (ρ_1, ρ_1^+) is created on I_1 as a result of the interaction), then we can conclude the lemma by following the same estimate as shown in Garavello and Piccoli (2006). If, on the other hand, a wave (ρ_1, ρ_1^+) is reflected then $\rho_1^- < \rho_1$, (ρ_1, ρ_1^-) is a rarefaction wave, and $f(\rho_1^-) \leq f(\rho_1^+) < \rho_1$. In other words, part of the change in the flow caused by the interaction passes through the junction, and part of it is reflected back onto I_1 . We may then apply the same argument as in Garavello and Piccoli (2006) to the part that passes through the junction ($f(\rho_1^+) - f(\rho_1^-)$) and conclude the lemma. □

Definition Appendix A.3. *If a ρ -wave from I_i interacts with the junction, producing a ρ -wave on link I_j , we call I_i and I_j the source and recipient of this interaction, respectively. Such an event is denoted $I_i \rightarrow I_j$.*

We observe that $|\xi_i(\rho_i^- - \rho_i)|$ is precisely the L^1 -distance of two initial conditions on I_i with and without the shift ξ_i at the discontinuity (ρ_i, ρ_i^-) . Similarly, $|\xi_j(\rho_j^+ - \rho_j^-)|$ is the L^1 -distance of the two solutions on I_j as a result of having or not having the initial shift ξ_i on I_i , respectively. Furthermore, if ξ_i is the only shift in the initial condition on I_i , then $|\xi_i(\rho_i^- - \rho_i)|$ is the norm of the tangent vector for I_i (see definition (A.2)) before the interaction, and $|\xi_j(\rho_j^+ - \rho_j^-)|$ is the norm of the tangent vector for I_j after the interaction. From (A.3), we have

$$|\xi_j(\rho_j^+ - \rho_j^-)| = \frac{|\Delta q_j|}{|\Delta q_i|} |\xi_i(\rho_i^- - \rho_i)| \quad (\text{A.4})$$

Therefore, to bound the norm of the tangent vectors one has to check that the multiplication factors $\frac{|\Delta q_j|}{|\Delta q_i|}$ remain uniformly bounded, regardless of the number of interactions that may occur at this junction.

Let us consider the diverge junction, and assume that a wave interacts with J from road I_i and produces a wave on road I_j , where $i, j = 1, 2, 3$. As in the proof of Lemma Appendix A.2, we can restrict to the flow passing through the junction (indeed the reflected part has the same flow variation and smaller shift since the reflected wave is a slow

big shock). According to (4.32), $\Delta q_2 = \alpha_{1,2}\Delta q_1$ and $\Delta q_3 = \alpha_{1,3}\Delta q_1$. Consequently, we have the following matrix of multiplication factors $\frac{|\Delta q_i|}{|\Delta q_j|}$:

$$\begin{aligned} \frac{|\Delta q_1|}{|\Delta q_1|} &= 1, & \frac{|\Delta q_2|}{|\Delta q_1|} &= \alpha_{1,2}, & \frac{|\Delta q_3|}{|\Delta q_1|} &= \alpha_{1,3}; \\ \frac{|\Delta q_1|}{|\Delta q_2|} &= \frac{1}{\alpha_{1,2}}, & \frac{|\Delta q_2|}{|\Delta q_2|} &= 1, & \frac{|\Delta q_3|}{|\Delta q_2|} &= \frac{\alpha_{1,3}}{\alpha_{1,2}}; \\ \frac{|\Delta q_1|}{|\Delta q_3|} &= \frac{1}{\alpha_{1,3}}, & \frac{|\Delta q_2|}{|\Delta q_3|} &= \frac{\alpha_{1,2}}{\alpha_{1,3}}, & \frac{|\Delta q_3|}{|\Delta q_3|} &= 1. \end{aligned} \quad (\text{A.5})$$

We denote this matrix by $\{Q_{ij}\}_{i,j=1,2,3}$. According to Garavello and Piccoli (2006), in order to estimate the tangent vector norm, it suffices to keep track of just one single shift and show the corresponding tangent vector norm is bounded regardless of the number of wave interactions. To this end, we consider the only meaningful sequence of wave interaction, which is of the form $I_i \rightarrow I_j, I_j \rightarrow I_k, \dots$. We observe that, if $\alpha_{1,2}$ and $\alpha_{1,3}$ are nonzero constants, then $Q_{ij}Q_{jk} = Q_{ik}$ for any $i, j, k = 1, 2, 3$. This means that no matter how many interactions occur, the multiplication factor is always an element of the matrix $\{Q_{ij}\}$ and is uniformly bounded. Thus the diverge model with fixed turning ratios is well posed. However, in the DNL model where $\alpha_{1,2}$ and $\alpha_{1,3}$ are time-varying, this is no longer true as we have shown in the counterexample in Section 4.2.1. The well-posedness requires some additional conditions to hold, and the corresponding proof needs more elaborated arguments that take into account the μ -waves. These will be done in Theorem 4.2.

Appendix B. Technical Proofs

Appendix B.1. Proof of Theorem 4.2

Proof. This proof is completed in several steps.

[Step 1]. We invoke the wave-front tracking framework and the generalized tangent vector to show the desired continuous dependence. As discussed in Appendix A.2, it boils down to showing that the increase in the tangent vector norm, as a result of arbitrary number of wave interactions (including both ρ -wave and μ -wave), remains bounded.

[Step 2]. First of all, the end of Appendix A.2 shows that, for constant values of μ (that is, with fixed vehicle turning ratios), the tangent vector norm is uniformly bounded regardless of the interactions between the ρ -waves and the junction. Next, one needs to consider the case where μ changes from one value to another, i.e. when a μ -wave interacts with the junction. In general, we consider two consecutive interaction times of the μ -waves: t_k and t_{k+1} , and let β_k be the multiplication factor for the tangent vector norm of ρ relative to the times t_k and t_{k+1} . More precisely, we have $v(t_{k+1}-) = \beta_k v(t_k+)$, where $v(t)$ is the tangent vector norm of ρ at time t . Clearly, β_k can only take value in the following matrix where $\alpha_{1,2}^k$ and $\alpha_{1,3}^k$ are given by the constant μ value during (t_k, t_{k+1}) ; see (A.5).

$$Q^k = \{Q_{ij}^k\} \doteq \begin{bmatrix} 1 & \alpha_{1,2}^k & \alpha_{1,3}^k \\ 1/\alpha_{1,2}^k & 1 & \alpha_{1,3}^k/\alpha_{1,2}^k \\ 1/\alpha_{1,3}^k & \alpha_{1,2}^k/\alpha_{1,3}^k & 1 \end{bmatrix}, \quad k = 0, 1, 2, \dots \quad (\text{B.1})$$

Similar arguments can be carried out to all other intervals $[t_{k+1}, t_{k+2}]$, $[t_{k+2}, t_{k+3}]$ and so forth. In the rest of the proof, our goal is to estimate the multiplication factor for the tangent norm of ρ under the WFT framework, assuming arbitrary interaction patterns of the ρ -waves and μ -waves.

[Step 3]. We define $\gamma \doteq \frac{\delta}{C_1} > 0$ where δ is stated in the hypothesis of this theorem and C_1 is the flow capacity of link I_1 . Without loss of generality, we let $\gamma < \frac{1}{2}$. Throughout **Step 3**, we assume that $\alpha_{1,2}(t) \geq \gamma$ and $\alpha_{1,3}(t) \geq \gamma$ (the other cases will be treated in **Step 4**).

As demonstrated at the end of Appendix A.2, in order to estimate the increase in the tangent vector norms it suffices to consider the following type of sequence in which ρ -waves interacts with the junction: $I_i \rightarrow I_j$ then $I_j \rightarrow I_k$; in other words, the recipient of the previous ρ -wave interaction is the source of the next ρ -wave interaction. For each $k \geq 1$, we let $I^{(k)} \in \{I_1, I_2, I_3\}$ be the recipient of the last interacting ρ -wave during (t_k, t_{k+1}) . This gives rise to the sequence $\{I^{(k)}\}_{k \geq 1}$; see Figure B.9 for an illustration.

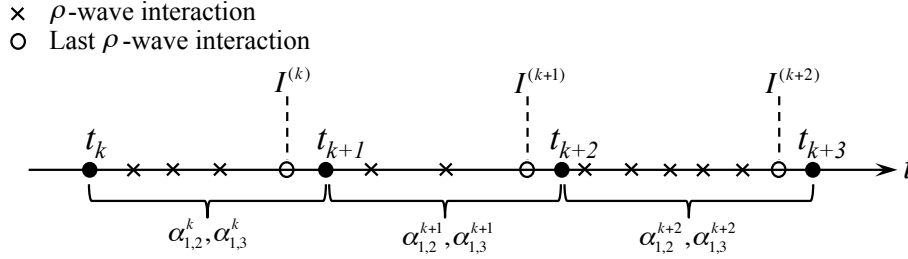


Figure B.9: t_k 's represent the times when μ -waves interact with the junction, changing the turning ratios $\alpha_{1,2}$ and $\alpha_{1,3}$. The crosses represent the times at which ρ -waves interact with the junction. The circles indicate the last ρ -wave interaction within the interval during which μ is constant. $I^{(k)}$'s denote the recipients of the last interacting ρ -waves.

We make the following crucial observation. Consider any three elements in the sequence of the form $I^{(k)} = I_i$, $I^{(k+1)} = I_2$ and $I^{(k+2)} = I_j$ where $i, j \in \{1, 2, 3\}$. By definition, the product of the multiplication factors within (t_{k+1}, t_{k+3}) is

$$Q_{i2}^{k+1} \cdot Q_{2j}^{k+2} = A_2^{k+1} \cdot Q_{ij}^l \quad \text{where} \quad A_2^{k+1} \in \left\{ 1, \frac{\alpha_{1,2}^{k+1}}{\alpha_{1,2}^{k+2}}, \frac{\alpha_{1,2}^{k+1}}{\alpha_{1,2}^{k+2}} \cdot \frac{\alpha_{1,3}^{k+2}}{\alpha_{1,3}^{k+1}} \right\}, \quad l \in \{k+1, k+2\} \quad (\text{B.2})$$

where we use the superscripts to indicate dependence on a specific time interval. The significance of (B.2) is that the multiplication factor can be decomposed into a term A_2 with a very specific structure (to be further elaborated below), and a term that would have been the multiplication factor as if the middle link $I_2 = I^{(k+1)}$ were removed. Clearly, the argument above applies equally to the case where $I^{(k+1)} = I_3$, and we use

$$A_3^{k+1} \in \left\{ 1, \frac{\alpha_{1,3}^{k+1}}{\alpha_{1,3}^{k+2}}, \frac{\alpha_{1,3}^{k+1}}{\alpha_{1,3}^{k+2}} \cdot \frac{\alpha_{1,2}^{k+2}}{\alpha_{1,2}^{k+1}} \right\}$$

to represent the term factored out if the middle link $I^{(k+1)} = I_3$ is removed. By repeating this procedure, one may eliminate all links I_2 and I_3 from the sequence $\{I^{(k)}\}$ except when they are the first or possibly the last in this sequence. As a result, the multiplicative terms $\{A_2^{k+1}\}$ and $\{A_3^{k+1}\}$ are factored out. Therefore, the entire multiplication factor for the tangent norm is bounded from above by

$$\prod_{m=1}^{\infty} A_2^{k_m+1} \cdot \prod_{n=1}^{\infty} A_3^{k_n+1} \cdot \frac{1}{\gamma^2} \quad (\text{B.3})$$

where $\{k_m\}_{m=1}^{\infty}$ and $\{k_n\}_{n=1}^{\infty}$ are subsequences of $\{k\}$ such that $I^{(k_m+1)} = I_2$ and $I^{(k_n+1)} = I_3$. The first two terms in (B.3) are results of eliminating I_2 and I_3 from the sequence $\{I^{(k)}\}$; the third term takes care of the first element and possibly the last element in the sequence, and is derived from the observation that $Q_{ij}^k \leq \frac{1}{\gamma}$ for all $i, j \in \{1, 2, 3\}$ and $k \geq 0$.

It remains to show that the first and second terms of (B.3) are bounded, and hence the entire (B.3) is bounded. We write, without referring explicitly to the multiplication indices, that

$$\prod_{m=1}^{\infty} A_2^{k_m+1} = \prod_k \frac{\alpha_{1,2}^{k+1}}{\alpha_{1,2}^{k+2}} \cdot \prod_k \frac{\alpha_{1,3}^{k+2}}{\alpha_{1,3}^{k+1}}$$

This leads to the following.

$$\begin{aligned} \prod_{m=1}^{\infty} A_2^{k_m+1} &= \exp\left(\sum_k \log \alpha_{1,2}^{k+1} - \log \alpha_{1,2}^{k+2}\right) \cdot \exp\left(\sum_k \log(1 - \alpha_{1,2}^{k+2}) - \log(1 - \alpha_{1,2}^{k+1})\right) \\ &\leq \exp\left(\sup_{\alpha \in [\gamma, 1-\gamma]} \frac{1}{|\alpha|} \cdot \sum_k |\alpha_{1,2}^{k+1} - \alpha_{1,2}^{k+2}|\right) \cdot \exp\left(\sup_{\alpha \in [\gamma, 1-\gamma]} \frac{1}{|1-\alpha|} \cdot \sum_k |\alpha_{1,2}^{k+2} - \alpha_{1,2}^{k+1}|\right) \\ &\leq \exp\left(\frac{1}{\gamma} \cdot TV(\mu)\right) \cdot \exp\left(\frac{1}{\gamma} \cdot TV(\mu)\right) < \infty \end{aligned}$$

where $TV(\mu)$ is the bounded total variation of the path disaggregation variable μ .

[Step 4]. In this part of the proof we deal with the situation where $\alpha_{1,2}(t) < \gamma$; the other case where $\alpha_{1,3}(t) < \gamma$ is entirely similar. We begin with the following observation.

$$f_1^{out}(t) = \min\left\{D_1(t), \frac{S_2(t)}{\alpha_{1,2}(t)}, \frac{S_3(t)}{\alpha_{1,3}(t)}\right\} = \min\left\{D_1(t), \frac{S_3(t)}{\alpha_{1,3}(t)}\right\}$$

since $\frac{S_2(t)}{\alpha_{1,2}(t)} > \frac{S_2(t)}{\gamma} = \frac{S_2(t)C_1}{\delta} \geq C_1 \geq D_1(t)$. In other words, the minimum is never attained at $\frac{S_2(t)}{\alpha_{1,2}(t)}$, and any ρ -wave interacting from I_2 will not generate new waves on I_1 or I_3 since $f_1^{out}(t)$ does not change before and after the interaction. So the only interactions that may change the tangent vector norm are $I_1 \rightarrow I_3$ and $I_3 \rightarrow I_1$, and the corresponding multiplication factors are respectively $\alpha_{1,3}(t)$ and $\frac{1}{\alpha_{1,3}(t)}$.

Consider any sequence of interaction times $\{t_k\}$ of the μ -waves. Since the interactions $I_1 \rightarrow I_1$ or $I_3 \rightarrow I_3$ do not generate any increase in the tangent norm, we only need to consider the following sequence of interactions: $\dots \rightarrow I_1 \rightarrow I_3 \rightarrow I_1 \rightarrow I_3 \dots$. The resulting multiplication factor is bounded by constant of the form

$$\prod_k \frac{\alpha_{1,3}^k}{\alpha_{1,3}^{k+1}} \cdot \left(\frac{1}{1-\gamma}\right)^2$$

where the second multiplicative term deals with the first and the last element in the sequence since $\max\{\alpha_{1,3}^k, \frac{1}{\alpha_{1,3}^k}\} = \frac{1}{\alpha_{1,3}^k} < \frac{1}{1-\gamma}$ for all k . We may then proceed in the same way as **Step 3** and conclude that this multiplication factor is bounded, provided that $TV(\mu) < \infty$. \square

Appendix B.2. Proof of Theorem 5.1

Proof. Since δ_k is defined in terms of the supplies, it suffices for us to focus only on those densities such that $\rho_i(t, x) > \rho_i^c$ for $I_i \in \tilde{\mathcal{A}}$, $(t, x) \in [0, T] \times [a_i, b_i]$. It is also useful to keep in mind that densities beyond the critical density always propagate backwards in space. The proof is divided into several steps.

[Step 1]. $k = 0$. We have $t \in [0, \frac{L}{\lambda})$. Since the network is initially empty, all the supplies $S_i(\rho_i(t, x))$, $I_i \in \tilde{\mathcal{A}}$, $(t, x) \in \{0\} \times [a_i, b_i]$, are maximal and equal to the respective flow capacities at $t = 0$. Afterwards, a higher-than-critical density or a lower-than-maximum supply can only emerge from the downstream end of a link and propagate backwards along this link. Moreover, these backward waves can never reach the upstream end of the link within $[0, \frac{L}{\lambda})$ since $\frac{L}{\lambda}$ is the minimum link traversal time for backward waves.

A higher-than-critical density (backward wave) can only arise in one of the following cases.

Case (1). A forward wave from I_1 (see Figure 4) interacts with the diverge junction and creates a backward wave on I_1 .

Case (2). A forward wave from I_4 (or I_5) interacts with the merge junction and creates a backward wave on I_4 or I_5 .

Case (3). A forward wave interacts with a destination from the relevant virtual link and creates a backward wave on the same virtual link.

Each individual case will be investigated in detail below.

- **Case (1).** We use the same notation shown in Figure 4. According to the reason provided above, $S_i(t) \equiv C_i$, $i = 2, 3$ for $t \in [0, \frac{L}{\lambda}]$. Let the time of the wave interaction be \bar{t} . Recall from (4.32) that

$$f_1^{out}(\bar{t}) = \min \left\{ D_1(\bar{t}), \frac{C_2}{\alpha_{1,2}(\bar{t})}, \frac{C_3}{\alpha_{1,3}(\bar{t})} \right\} \quad (\text{B.4})$$

If the minimum is attained at $D_1(\bar{t})$, then the entrance of I_1 will remain in the uncongested phase, i.e. $\rho_1(t+, b_1-) \leq \rho_1^c$ after the interaction. Hence, no lower-than-maximum supply is generated. On the other hand, if say $\frac{C_2}{\alpha_{1,2}(\bar{t})}$ is the smallest among the three, then

$$S_1(\rho_1(\bar{t}+, b_1-)) \geq f_1(\rho_1(\bar{t}+, b_1-)) = f_1^{out}(\bar{t}+) = \frac{C_2}{\alpha_{1,2}(\bar{t}+)} \geq C_2 \geq C^{min} \quad (\text{B.5})$$

In summary, the supply values corresponding to the backward waves generated at I_1 , if any, are uniformly above C^{min} .

- **Case (2).** We turn to the merge junction shown in Figure 4, and note $S_6(t) \equiv C_6$ for $t \in [0, \frac{L}{\lambda}]$. As usual, we let \bar{t} be the time of interaction. There are two further cases for the merge junction model as shown in Figure 5. We first consider the situation illustrated in Figure 5(a). Clearly, we have that

$$S_4(\rho_4(\bar{t}+, b_4-)) \geq f_4(\rho_4(\bar{t}+, b_4-)) = f_4^{out}(\bar{t}+) = pC_6 \geq \bar{p}C^{min} \quad (\text{B.6})$$

$$S_5(\rho_5(\bar{t}+, b_5-)) \geq f_5(\rho_5(\bar{t}+, b_5-)) = f_5^{out}(\bar{t}+) = (1-p)C_6 \geq \bar{p}C^{min} \quad (\text{B.7})$$

That is, the supply values of the backward waves generated at the downstream ends of I_4 and I_5 are uniformly above $\bar{p}C^{min}$.

For the situation depicted in Figure 5(b), we first note that the coordinates of Q' is $(pC_6, (1-p)C_6)$, and the coordinates of the solution $Q = (f_4^{out,*}, f_5^{out,*})$ either satisfy

$$f_4^{out,*} < pC_6 \quad \text{and} \quad f_5^{out,*} > (1-p)C_6 \quad (\text{B.8})$$

as shown exactly in Figure 5(b), or

$$f_4^{out,*} > pC_6 \quad \text{and} \quad f_5^{out,*} < (1-p)C_6 \quad (\text{B.9})$$

Taking (B.8) as an example (the (B.9) case can be treated similarly), we have

$$S_5(\rho_5(\bar{t}+, b_5-)) \geq f_5(\rho_5(\bar{t}+, b_5-)) > (1-p)C_6 \geq \bar{p}C^{min}; \quad (\text{B.10})$$

and no increase in density is produced at the downstream end of link I_4 since its exit flow is equal to the demand.

To sum up, the supply values corresponding to the backward waves generated at I_4 or I_5 , if any, are uniformly above $\bar{p}C^{min}$.

- **Case (3).** For each destination $d \in \mathcal{D}$, let S^d be its supply and denote by vl the virtual link connected to d . If $S^d \geq C_{vl}$ then no backward waves can be generated on this link and the supply value on the link is always equal to C_{vl} . If $S^d < C_{vl}$, then only one higher-than-critical density can exist on this virtual link, that is, ρ such that $\rho > \rho_{vl}^c$ and $f_{vl}(\rho) = S^d$. Clearly, its supply value is equal to S^d .

To sum up, the supply value corresponding to the backward waves generated at any virtual link, if any, is bounded below by $\delta^{\mathcal{D}}$.

Finally, we notice that all the backward waves exhaustively described above originate from the downstream end of a link, and they cannot reach the upstream end of the same link within period $[0, \frac{L}{\lambda}]$. Thus, these backward waves cannot bring further reduction in the supply values by means of interacting with the junctions. We conclude that during period $[0, \frac{L}{\lambda}]$, the minimum supply in the network, δ_0 , is bounded below; that is,

$$\delta_0 \geq \min \{ \delta^{\mathcal{D}}, \bar{p}C^{min} \} \quad (\text{B.11})$$

[Step 2]. We move on to $k \geq 1$. In addition to Case (1)-(3), which do not bring any supply values below $\min\{\delta^D, \bar{p}C^{min}\}$, two more cases may arise in which higher-than-critical densities may be generated as a result of backward waves interacting with junctions:

Case (4). A backward wave from I_2 (or I_3 , see Figure 4) interacts with the diverge junction and creates a backward wave in I_1 .

Case (5). A backward wave from I_6 (see Figure 4) interacts with the merge junction and creates a backward wave in I_4 or I_5 .

Case (4) and Case (5) are analyzed in detail below.

- **Case (4).** Without loss of generality, we assume that the backward wave that interacts with the diverge junction is coming from I_2 , and has the density value $\rho_2^- \in (\rho_2^c, \rho_2^{jam}]$. Let \bar{t} be the time of the interaction. In view of (B.4), if the minimum is attained at $D_1(\bar{t})$, then the interaction does not bring any increase in density at the downstream end of I_1 , hence no decrease in the supply there.

If the minimum is attained at $\frac{S_2(\bar{t})}{\alpha_{1,2}(\bar{t})}$, we deduce in a similar way as (B.5) that

$$S_1(\rho_1(\bar{t}+, b_1-)) \geq f_1(\rho_1(\bar{t}+, b_1-)) = f_1^{out}(\bar{t}+) = \frac{S_2(\rho_2^-)}{\alpha_{1,2}(\bar{t}+)} \geq S_2(\rho_2^-) \geq \delta_{k-1}$$

The last inequality is due to the fact that a backward wave such as ρ_2^- must be created at the downstream end of I_2 at a time earlier than $k\frac{L}{\lambda}$, thus its supply value $S_2(\rho_2^-)$ must be bounded below by δ_{k-1} . If the minimum is attained at $\frac{S_3(\bar{t})}{\alpha_{1,3}(\bar{t})}$, we have

$$S_1(\rho_1(\bar{t}+, b_1-)) \geq f_1(\rho_1(\bar{t}+, b_1-)) = f_1^{out}(\bar{t}+) = \frac{S_3(\bar{t})}{\alpha_{1,3}(\bar{t}+)} \geq S_3(\bar{t}+) \geq \delta_{k-1}$$

The last inequality is because any lower-than-maximum supply on I_3 must be created in the previous time interval.

To sum up, the supply values corresponding to the backward waves generated at I_1 , if any, are bounded below by δ_{k-1} .

- **Case (5).** For the merge junction, we begin with the case illustrated in Figure 5(a). Assuming the backward wave that interacts with the merge junction from I_6 has the density value $\rho_6^- \in (\rho_6^c, \rho_6^{jam}]$. Similar to (B.6)-(B.7), we have

$$S_4(\rho_4(\bar{t}+, b_4-)) \geq f_4(\rho_4(\bar{t}+, b_4-)) = f_4^{out}(\bar{t}+) = pS_6(\rho_6^-) \geq \bar{p}\delta_{k-1} \quad (\text{B.12})$$

$$S_5(\rho_5(\bar{t}+, b_5-)) \geq f_5(\rho_5(\bar{t}+, b_5-)) = f_5^{out}(\bar{t}+) = (1-p)S_6(\rho_6^-) \geq \bar{p}\delta_{k-1} \quad (\text{B.13})$$

where the last inequalities are due to the same reason provided in **Case (4)**. The case illustrated in Figure 5(b) can be treated in the same way as (B.8)-(B.10).

To sum up, the supply values corresponding to the backward waves generated at I_4 or I_5 , if any, must be bounded below by $\bar{p}\delta_{k-1}$.

So far, we have shown that for $t \in [k\frac{L}{\lambda}, (k+1)\frac{L}{\lambda})$ where $k \geq 1$, the presence of higher-than-critical densities, as exhaustively illustrated through **Case (1)- Case (5)**, brings supply values throughout the entire network that are bounded below by

$$\min \left\{ \underbrace{\min\{\delta^D, \bar{p}C^{min}\}}_{\text{Case (1)-(3)}}, \underbrace{\delta_{k-1}}_{\text{Case (4)}}, \underbrace{\bar{p}\delta_{k-1}}_{\text{Case(5)}} \right\} = \min\{\delta^D, \bar{p}C^{min}, \bar{p}\delta_{k-1}\} = \min\{\delta^D, \bar{p}\delta_{k-1}\} \quad (\text{B.14})$$

[Step 3]. Recall (B.11) and (B.14):

$$\delta_0 \geq \min\{\delta^D, \bar{p}C^{min}\}, \quad \delta_k \geq \min\{\delta^D, \bar{p}\delta_{k-1}\} \quad \forall k \geq 1 \quad (\text{B.15})$$

We define $\hat{\delta}_0 \doteq \min\{\delta^{\mathcal{D}}, \bar{p}C^{\min}\}$ and $\hat{\delta}_k \doteq \min\{\delta^{\mathcal{D}}, \bar{p}\hat{\delta}_{k-1}\}$, $k \geq 1$. Clearly, $\bar{p}\hat{\delta}_{k-1} \leq \delta^{\mathcal{D}}$ for all $k \geq 1$, which implies that $\hat{\delta}_k = \min\{\delta^{\mathcal{D}}, \bar{p}\hat{\delta}_{k-1}\} = \bar{p}\hat{\delta}_{k-1}$, $\forall k \geq 1$. Thus

$$\delta_0 \geq \hat{\delta}_0 = \min\{\delta^{\mathcal{D}}, \bar{p}C^{\min}\}, \quad \delta_k \geq \hat{\delta}_k = \bar{p}\hat{\delta}_{k-1} = \bar{p}^k \hat{\delta}_0 = \bar{p}^k \min\{\delta^{\mathcal{D}}, \bar{p}C^{\min}\} \quad \forall k \geq 1$$

□

Appendix B.3. Proof of Lemma 5.4

Proof. The proof is divided into a few steps.

[Step 1]. Notice that assumption 3 implies that the departure rates $\{h_p(\cdot), p \in \mathcal{P}\}$ are non-zero on a finite set of intervals. Indeed, let n be the number of intervals where $h_p(\cdot)$ does not vanish then $n\epsilon \leq TV(h_p) < \infty$, which implies that n is finite.

[Step 2]. Using the assumption that each fundamental diagram $f_i(\cdot)$ has nonvanishing derivative, we have, at each origin, that the bounded total variation of the density must imply bounded total variation of the flow, and vice versa. Therefore, the assumption on the bounded variation of $h_p(\cdot)$ implies that the density and path disaggregation variable are of bounded variation on the virtual link incident to that origin.

[Step 3]. Assumption 1 guarantees that, on each link, all waves of the type $(0, \rho)$ or $(\rho, 0)$ are contact discontinuities for ρ sufficiently small and, in particular, travel with a constant speed. Moreover, all μ -waves travel with the same speed for low densities. Therefore, taking into account **Step 1**, whenever μ is non-zero, it is uniformly bounded away from zero on the entire network. In particular there exists $\epsilon' > 0$ so that $\mu_i^p(t, x) \in \{0\} \cup [\epsilon', 1]$ for every t, x, i and p . Therefore, at diverging junctions, the coefficients $\alpha_{1,2}(t)$ and $\alpha_{1,3}(t)$ satisfy the same properties.

[Step 4]. Let us now turn to the total variation of the path disaggregation variables. We know, from **Step 2**, that μ has bounded variation on virtual links incident to the origins. We also know from **Step 3** that μ is bounded away from zero whenever it is non-zero; and the same holds for the turning ratios at diverge junctions. Consider a μ -wave (μ_l, μ_r) , then its variation $|\mu_l - \mu_r|$ can change only upon interaction with diverge junctions. More precisely, denote by (μ_l^-, μ_r^-) and (μ_l^+, μ_r^+) the wave respectively before and after the interaction, we have $|\mu_l^+ - \mu_r^+| \leq \frac{1}{\alpha} |\mu_l^- - \mu_r^-|$ where $\alpha = \alpha_{1,2}$ or $\alpha = \alpha_{1,3}$ and is bounded away from zero. Since the μ -waves travel only forward on the links with uniformly bounded speed, we must have that the interactions with diverge junctions can occur only finite number of times. Thus we conclude that μ has bounded total variation. □

Appendix B.4. Proof of Lemma 5.6

Proof. Let ζ_p^j be the shift of the j -th jump of $h_p(\cdot)$, which occurs at time t_j , then the expression of $q_s(\cdot)$ is possibly affected on the interval $[t_j, t_j + \zeta_p^j]$ (assuming $\zeta_p^j > 0$). More precisely, if $q_s(\bar{t}) > 0$ then no wave is generated on the virtual link while a shift in the queue is generated with $\eta_s = \Delta_j h_p \cdot \zeta_p^j$, where $\Delta_j h_p$ is the jump in $h_p(\cdot)$ occurring at time t_j . On the other hand, if $q_s(\bar{t}) = 0$ then a wave (ρ^-, ρ^+) is produced at time t_j on the virtual link with shift $\xi_\rho^i = \lambda \cdot \zeta_p^j$ where λ is the speed of the wave (ρ^-, ρ^+) . We can then compute:

$$\xi_\rho^i \cdot (\rho^+ - \rho^-) = \zeta_p^j \cdot \lambda \cdot (\rho^+ - \rho^-) = \zeta_p^j \cdot \frac{f(\rho^+) - f(\rho^-)}{\rho^+ - \rho^-} \cdot (\rho^+ - \rho^-)$$

Moreover, $f(\rho^+) - f(\rho^-) = \Delta_j h_p$, thus the norm of the tangent vector generated is the same as before.

To prove that the norm of the tangent vector $(\eta_s, \xi_\rho^i, \xi_\mu^{i,p})$ is bounded for all times, let us first consider a backward-propagating wave (ρ^-, ρ^+) interacting with the queue q_s , and with a shift ξ_ρ^i . Then we can write:

$$\dot{q}_s^+ - \dot{q}_s^- = f(\rho^-) - f(\rho^+)$$

where \dot{q}_s^- and \dot{q}_s^+ are the time-derivatives of $q_s(\cdot)$ before and after the interaction, respectively. Therefore, denoting λ the speed of the wave (ρ^-, ρ^+) , we get:

$$\eta_s = \frac{\xi_\rho^i}{\lambda} \cdot (f(\rho^-) - f(\rho^+)) = \frac{\xi_\rho^i \cdot (\rho^- - \rho^+)}{f(\rho^-) - f(\rho^+)} \cdot (f(\rho^-) - f(\rho^+)) = \xi_\rho^i \cdot (\rho^- - \rho^+)$$

Thus the norm of the tangent vector is bounded.

The norm of the tangent vector $(\eta_s, \xi_\rho^i, \xi_\mu^{i,p})$ may also change when the queue q_s becomes empty, but this can be treated in the same way as in Herty et al. (2007). \square

References

- Aboudolas, K., Papageorgiou, M., Komsmatopoulous, E., 2009. Store-and-forward based methods for the signal control problem in large-scale congested urban road networks. *Transportation Research Part C*, 17 (2), 163-174.
- Bressan, A., 1993. A contractive metric for systems of conservation laws with coinciding shock and rarefaction curves. *Journal of Differential Equations* 106, 332 - 366.
- Bressan, A., 2000. *Hyperbolic Systems of Conservation Laws. The One Dimensional Cauchy Problem*. Oxford University Press.
- Bressan, A., Crasta, G., Piccoli, B., 2000. Well-posedness of the Cauchy problem for $n \times n$ systems of conservation laws. *Memoirs of the American Mathematical Society* 694.
- Bressan, A., Han, K., 2011. Optima and equilibria for a model of traffic flow. *SIAM Journal on Mathematical Analysis* 43 (5), 2384-2417.
- Bressan, A., Han, K., 2013. Existence of optima and equilibria for traffic flow on networks. *Networks and Heterogeneous Media*, 8 (3), 627-648.
- Continuous Riemann solvers for traffic flow at a junction. *Discrete and Continuous Dynamical Systems - Series A* 35 (9), 4149-4171.
- Coclite, G.M., Garavello, M., Piccoli, B., 2005. Traffic flow on a road network. *SIAM Journal on Mathematical Analysis* 36 (6), 1862-1886.
- Colombo, R.M., Goatin, P., Piccoli, B., 2010. Road networks with phase transitions. *Journal of Hyperbolic Differential Equations* 7 (1), 85-106.
- Dafermos, C.M., 1972. Polygonal approximations of solutions of the initial value problem for a conservation law. *Journal of Mathematical Analysis and Applications* 38 (1), 33-41.
- Daganzo, C.F., 1994. The cell transmission model. Part I: A simple dynamic representation of highway traffic. *Transportation Research Part B* 28 (4), 269-287.
- Daganzo, C.F., 1995. The cell transmission model. Part II: Network traffic. *Transportation Research Part B* 29 (2), 79-93.
- Daganzo, C.F., 2006. On the variational theory of traffic flow: well-posedness, duality and application. *Network and heterogeneous media* 1 (4), 601-619.
- Friesz, T.L., Bernstein, D., Smith, T., Tobin, R., Wie, B., 1993. A variational inequality formulation of the dynamic network user equilibrium problem. *Operations Research* 41 (1), 80-91.
- Friesz, T.L., Han, K., Neto, P.A., Meimand, A., Yao, T., 2013. Dynamic user equilibrium based on a hydrodynamic model. *Transportation Research Part B* 47 (1), 102-126.
- Garavello, M., Piccoli, B., 2006. *Traffic Flow on Networks. Conservation Laws Models*. AIMS Series on Applied Mathematics, Springfield, Mo..
- Garavello, M., Piccoli, B., 2006. Traffic flow on a road network using the Aw-Rascle model. *Communications in Partial Differential Equations* 31 (1), 243-275.
- Gazis, D.C and Potts, R.B., 1963. The oversaturated intersection. In the proceedings of the Second International Symposium on Traffic Theory, London, UK.
- Godunov, S.K., 1959. A difference scheme for numerical solution of discontinuous solution of hydrodynamic equations. *Math Sbornik* 47 (3), 271-306.
- Godvik, M.; Hanche-Olsen, H., 2008. Existence of solutions for the Aw-Rascle traffic flow model with vacuum. *Journal of Hyperbolic Differential Equations* 5 (1), 45-63.
- Han, D., Lo, H.K., 2002. Two new self-adaptive projection methods for variational inequality problems. *Computers and Mathematics with Applications* 43, 1529-1537.
- Han, D., Lo, H.K., 2003. Solving Non-additive Traffic Assignment Problems: A Decent Methods for Co-coercive Variational Inequalities. *European Journal of Operational Research*, 159(3), 529-544.
- Han, K., Friesz, T.L., Szeto, W.Y., Liu, H., 2015a. Elastic demand dynamic network user equilibrium: Formulation, existence and computation. *Transportation Research Part B*, DOI: 10.1016/j.trb.2015.07.008.
- Han, K., Friesz, T.L., Yao, T., 2012. Continuity of the effective delay operator for networks based on the link delay model. arXiv:1211.4621.
- Han, K., Friesz, T.L., Yao, T., 2013a. A partial differential equation formulation of Vickrey's bottleneck model, part I: Methodology and theoretical analysis. *Transportation Research Part B* 49, 55-74.
- Han, K., Friesz, T.L., Yao, T., 2013b. A partial differential equation formulation of Vickrey's bottleneck model, part II: Numerical analysis and computation. *Transportation Research Part B* 49, 75-93.
- Han, K., Friesz, T.L., Yao, T., 2013c. Existence of simultaneous route and departure choice dynamic user equilibrium. *Transportation Research Part B* 53, 17-30.
- Han, K., Gayah, V., Piccoli, B., Friesz, T.L., Yao, T., 2014. On the continuum approximation of the on-and-off signal control on dynamic traffic networks. *Transportation Research Part B* 61, 73-97.
- Han, K., Gayah, V., 2015. Continuum signalized junction model for dynamic traffic networks: Offset, spillback, and multiple signal phases. *Transportation Research Part B* 77, 213-239.
- Han, K., Piccoli, B., Szeto, W.Y., 2015b. Continuous-time link-based kinematic wave model: formulation, solution existence, and well-posedness. *Transportmetrica B: Transport Dynamics*, DOI: 10.1080/21680566.2015.1064793.

- Haut, B., Bastin, G., 2007. A second order model of road junctions in fluid models of traffic networks. *Networks and Heterogeneous Media* 2 (2), 227-253.
- Herty, M., Rascle, M., 2006. Coupling conditions for a class of second-order models for traffic flow. *SIAM Journal on Mathematical Analysis* 38 (2), 595-616.
- Herty, M., Klar, A., Piccoli, B., 2007. Existence of solutions for supply chain models based on partial differential equations, *SIAM J. Math. Anal.* 39, 160173.
- Holden, H., Risebro, N.H., 1995. A mathematical model of traffic flow on a network of unidirectional roads, *SIAM Journal on Mathematical Analysis* 26 (4), 999-1017.
- Holden, H., Risebro, N.H., 2002. *Front Tracking for Hyperbolic Conservation Laws*. Springer.
- Huang, H.J., Lam, W.H.K., 2002. Modeling and solving dynamic user equilibrium route and departure time choice problem in network with queues. *Transportation Research Part B* 36, 253-273.
- Jin, W.-L., 2010. Continuous kinematic wave models of merging traffic flow. *Transportation Research Part B* 44 (8-9), 1084-1103.
- Jin, W.-L., Zhang, H.M., 2003. On the distribution schemes for determining flows through a merge. *Transportation Research Part B* 37 (6), 521-540.
- Larsson, S., Thomée, V., 2005. *Partial Differential Equation with Numerical Methods*. Springer-Verlag Berlin and Heidelberg GmbH & Co. K.
- Lebacque, J., Khoshyaran, M., 1999. Modeling vehicular traffic flow on networks using macroscopic models, in *Finite Volumes for Complex Applications II*, 551-558, Hermes Science Publications, Paris.
- LeVeque, R.J., 1992. *Numerical Methods for Conservation Laws*. Birkhäuser.
- Lighthill, M., Whitham, G., 1955. On kinematic waves. II. A theory of traffic flow on long crowded roads. *Proceedings of the Royal Society of London: Series A* 229 (1178), 317-345.
- Lu C., Zhou, X. Zhang, K., 2013. Dynamic origin-destination demand flow estimation under congested traffic conditions. *Transportation Research Part C* 34, 16-37.
- Peeta, S., Ziliaskopoulos, A.K., 2001. Foundations of dynamic traffic assignment: The past, the present and the future. *Networks and Spatial Economics* 1, 233-265.
- Richards, P.I., 1956. Shockwaves on the highway. *Operations Research* 4 (1), 42-51.
- Smith, M.J., Wisten, M.B., 1995. A continuous day-to-day traffic assignment model and the existence of a continuous dynamic user equilibrium. *Annals of Operations Research* 60 (1), 59-79.
- Szeto, W.Y., 2003. *Dynamic Traffic Assignment: Formulations, properties, and extensions*. PhD Thesis, The Hong Kong University of Science and Technology, China.
- Ukkusuri, S., Han, L., Doan, K., 2012. Dynamic user equilibrium with a path based cell transmission model for general traffic networks. *Transportation Research Part B* 46 (10), 1657-1684.
- Vickrey, W.S., 1969. Congestion theory and transport investment. *The American Economic Review* 59 (2), 251-261.
- Wie, B. W., Tobin R. L., Carey, M., 2002. The existence, uniqueness and computation of an arc-based dynamic network user equilibrium formulation. *Transportation Research Part B* 36, 897-918.
- Yperman, I., Logghe, S., Immers, L., 2005. The link transmission model: An efficient implementation of the kinematic wave theory in traffic networks, *Advanced OR and AI Methods in Transportation, Proc. 10th EWGT Meeting and 16th Mini-EURO Conference*, Poznan, Poland, 122-127, Publishing House of Poznan University of Technology.
- Zhu, D.L., Marcotte, P., 2000. On the existence of solutions to the dynamic user equilibrium problem. *Transportation Science* 34 (4), 402-414.